

# Modelling Function-Valued Processes with Nonseparable Covariance Structure

Evandro Konzen<sup>1</sup>, Jian Qing Shi<sup>1\*</sup> and Zhanfeng Wang<sup>2</sup>

<sup>1</sup>School of Mathematics, Statistics & Physics, Newcastle University, UK

<sup>2</sup>Department of Statistics and Finance, Management School, University of Science and Technology of China, Hefei, China.

4th June 2022

## Abstract

We discuss a general Bayesian framework on modelling multidimensional function-valued processes by using a Gaussian process or a heavy-tailed process as a prior, enabling us to handle nonseparable and/or nonstationary covariance structure. The nonstationarity is introduced by a convolution-based approach through a varying kernel, whose parameters vary along the input space and are estimated via a local empirical Bayesian method. For the varying anisotropy matrix, we propose to use a spherical parametrisation, leading to unconstrained and interpretable parameters. The unconstrained nature allows the parameters to be modelled as a nonparametric function of time, spatial location or other covariates. Furthermore, to extract important information in data with complex covariance structure, the Bayesian framework can decompose the function-valued processes using the eigenvalues and eigensurfaces calculated from the estimated covariance structure. The results are demonstrated by simulation studies and by an application to real data.

**Keywords:** Covariance separability; Function-valued process; Gaussian process; Nonstationary covariance structure; Unconstrained parametrisation

## 1 Introduction

In multidimensional (or multiway) functional data analysis, we assume that the observed data are realisations of an underlying random process  $X(\mathbf{t})$ ,  $\mathbf{t} \in \mathcal{T} \subset \mathbb{R}^Q$ , which has mean function  $\mu(\mathbf{t})$  and covariance function  $k(\mathbf{t}, \mathbf{t}') = \text{Cov}[X(\mathbf{t}), X(\mathbf{t}')].$

The accurate estimate of the covariance function, which is one of the key steps in functional principal components analysis (FPCA) and other inference methods for functional data analysis

---

\*Corresponding author, email: j.q.shi@ncl.ac.uk

(Ramsay and Silverman, 2005), is a challenging task. When the dimension of the input space is  $Q = 2$ , the covariance function depends on four arguments and, in the case of sparse designs, nonparametric estimation may suffer from the curse of dimensionality and slow computing. These difficulties are rapidly aggravated as  $Q$  becomes larger.

In order to address these issues, many models for two-way functional data (e.g. Chen and Müller (2012); Allen et al. (2014); Chen et al. (2017)) and spatiotemporal data (Banerjee et al. (2015) and references therein) assume that the covariance function  $k(\mathbf{t}, \mathbf{t}')$  is separable. In other words, they assume that the covariance function can be factorised into the product between  $Q$  covariance functions, each one corresponding to one direction.

Besides reducing computational costs and offering attractive interpretation, the separability assumption is also useful because it makes easier to guarantee positive definiteness of the covariance function. However, it does not allow any interaction between the inputs in the covariance structure, and this motivated the recent interest in developing hypothesis tests for separability (Aston et al., 2017; Constantinou et al., 2017; Cappello et al., 2018).

Although general classes of nonseparable covariance functions were proposed almost two decades ago (Cressie and Huang, 1999; Gneiting, 2002; De Iaco et al., 2002; Stein, 2005), they are restricted to the scope of stationarity.

In this paper, we discuss a general Bayesian framework on modelling function-valued processes by using a Gaussian process (GP) or other heavy-tailed processes as a prior, allowing nonseparable and/or nonstationary covariance structure. The nonstationarity is defined by a convolution-based approach (Higdon et al., 1999) via a varying kernel. In the case of Gaussian kernel, the nonstationary covariance structure can be simply defined by a varying anisotropy matrix. A local empirical Bayesian approach is used to estimate the hyperparameters involved in the models, including both fixed and varying coefficients.

The Bayesian framework provides an efficient approach for obtaining predictive distribution for the unknown underlying regression functions of the processes; in the meantime, it can also decompose the function-valued processed using the eigenvalues and eigensurfaces calculated from the estimated covariance structure. A finite number of the eigensurfaces can be used to extract some most important and interpretable information involved in different types of data with complex structure in the spirit of functional principal component analysis. Nonstationarity and interaction among the coordinates of the input can be captured via this flexible approach.

In Section 2, we will give a brief introduction on how to define a Bayesian process model for function-valued processes, followed by defining nonstationary covariance structure by a varying kernel or a varying anisotropy matrix in the case of Gaussian kernel via a convolution based approach. A parametrisation method will be discussed and used to model the varying anisotropy matrix, and a local Empirical Bayesian approach will be used to estimate all the hyperparameters included in the covariance structure. The predictive distribution and decomposition of the random processes are discussed in Section 3. Some asymptotic theory will also be provided in the section. Simulation studies and real data examples are presented in Section 4 and 5. Finally, we will give a brief discussion in Section 6.

## 2 Function-valued processes with nonseparable and/or nonstationary covariance structure

### 2.1 Bayesian process models

Let us consider the following nonlinear functional regression model or a process regression model:

$$X(\mathbf{t}) = f(\mathbf{t}) + \varepsilon(\mathbf{t}), \quad \varepsilon(\mathbf{t}) \sim N(0, \sigma_\varepsilon^2), \quad (1)$$

where  $\mathbf{t} \in \mathcal{T} \subset \mathbb{R}^Q$  and the unknown nonlinear regression function  $f$  is a mapping  $f(\cdot) : \mathbb{R}^Q \rightarrow \mathbb{R}$ . The additive noise  $\varepsilon(\mathbf{t})$  is assumed to have normal distribution, but it could have a different distribution (e.g. generalised Gaussian process regression models in Wang and Shi (2014)).

A variety of models has been proposed to estimate the unknown function  $f$ . Popular models are based on the approximation  $f(\mathbf{t}) = \sum_{j=1}^J \alpha_j \phi_j(\mathbf{t})$ , where  $\phi_j$  are basis functions (e.g. smoothing splines (Wahba, 1990)). One of the major difficulties of these frequentist approaches is the *curse of dimensionality* problem in the estimation process when  $\mathbf{t}$  is multidimensional.

From the Bayesian perspective, the function  $f$  is treated as an unknown process (an unknown random function defined in a functional space analogue of a random unknown parameter defined in a conventional Bayesian approach). Therefore, we need to specify a prior distribution over the (random) function  $f$  to make probabilistic inference about  $f$ . One way to do that is by using a Gaussian process (GP) prior.

The Gaussian process (see e.g. O’Hagan and Kingman (1978); Rasmussen and Williams (2006); Shi and Choi (2011)) is defined as a stochastic process parametrised by its mean function

$$\mu(\cdot) : \mathcal{T} \rightarrow \mathbb{R}, \quad \mu(\mathbf{t}) = E[f(\mathbf{t})],$$

and its covariance function

$$k(\cdot, \cdot) : \mathcal{T}^2 \rightarrow \mathbb{R}, \quad k(\mathbf{t}, \mathbf{t}') = \text{Cov}[f(\mathbf{t}), f(\mathbf{t}')].$$

From now on, we will write the GP as

$$f(\cdot) \sim GP(\mu(\cdot), k(\cdot, \cdot)). \quad (2)$$

GP can be seen as a generalisation of the multivariate Gaussian distribution to the infinite-dimensional case. When we use a GP prior (2) for the random function  $f$ , (1) is referred to as Gaussian process regression (GPR) model. In this case, for any finite  $n$  and  $\mathbf{t}_1, \dots, \mathbf{t}_n \in \mathcal{T}$ , the joint distribution of  $\mathbf{x} = (x(\mathbf{t}_1), \dots, x(\mathbf{t}_n))^T$  in eq. (1) is an  $n$ -variate Gaussian distribution with mean vector  $\boldsymbol{\mu} = (\mu(\mathbf{t}_1), \dots, \mu(\mathbf{t}_n))^T$  and covariance matrix  $\boldsymbol{\Psi}_n$  whose  $(i, j)$ -th entry is given by  $[\boldsymbol{\Psi}_n]_{ij} = k(\mathbf{t}_i, \mathbf{t}_j) + \delta_{ij}\sigma_\varepsilon^2$ ,  $i, j = 1, \dots, n$ , where  $\delta_{ij} = 1$  if  $i = j$  and 0 otherwise.

As we will focus on the covariance structure, we will use the mean function estimated via local linear smoother as it is commonly made in FDA (e.g. Yao et al. (2005)). Other mean models can also be used.

GPR models have become popular for a number of reasons. Firstly, a wide class of nonlinear functions  $f$  can be modelled by choosing a suitable prior specification for  $k(\cdot, \cdot)$ . Other prior

distributions can be used for robust heavy-tailed processes (Shah et al., 2014; Wang et al., 2017; Cao et al., 2018). This enables us to estimate the covariance structure directly based on the data. In addition, the applicability of GPR models can be readily extended to random process defined on dimensions higher than two. Finally, these models allow to easily quantify the variability of predictions.

Many recent developments have been made in GPR analysis, including variational GP (Tran et al., 2015), distributed GP (Deisenroth and Ng, 2015), manifold GP (Calandra et al., 2016), linearly constrained GP (Jidling et al., 2017), convolutional GP (van der Wilk et al., 2017), and deep GP (Dunlop et al., 2018). Some studies investigate connections between GPs with frequentist kernel methods based on reproducing kernel Hilbert spaces (Kanagawa et al., 2018). Finally, many extensions and adaptations have been suggested to apply GPR models to different types of data, such as big data (Liu et al., 2018), binary times series (Sung et al., 2017), large spatial data (Zhang et al., 2019), and mixed functional and scalar data in nonparametric functional regression (Wang and Xu, 2019).

The covariance function  $k(\mathbf{t}, \mathbf{t}')$  plays a key role in the Bayesian process models (1) and (2). When the input  $\mathbf{t}$  is one- or two-dimensional, we can use either a nonparametric covariance (see e.g. Hall et al., 2008) or a parametric one. A typical parametric stationary covariance function for the random process  $X(\mathbf{t}) = f(\mathbf{t}) + \varepsilon(\mathbf{t})$  is of the form

$$\text{Cov}[X(\mathbf{t}), X(\mathbf{t} + \mathbf{h})] = \sigma^2 g(\sqrt{\mathbf{h}^\top \mathbf{B} \mathbf{h}}) + \sigma_\varepsilon^2 \delta_{\mathbf{h}}, \quad (3)$$

where  $g$  is a valid correlation function,  $B$  is the anisotropy matrix, and  $\delta_{\mathbf{h}} = 1$  if  $\mathbf{h} = \mathbf{0}$  and  $\delta_{\mathbf{h}} = 0$  otherwise. Suppose that  $B = \text{diag}(b_1, \dots, b_Q)$ . The hyperparameters  $\sigma^2$ ,  $\sigma_\varepsilon^2$  and  $1/b_q$  are called the signal variance, the noise variance and the length-scale parameters, respectively. In spatial statistics, these hyperparameters are called the *partial sill*, the *nugget effect* and the *range* parameters, respectively (Banerjee et al., 2015). The value of  $\sigma^2$  controls the vertical scale of variation of  $f$ .

The diagonal elements of  $B$ , usually called decay parameters, control how quickly the function  $f$  varies on each coordinate direction. The larger the value, the quicker is the variation of  $f$  towards the related direction. The off-diagonal elements of  $B$  may be non-zero. If  $b_{pq} \neq 0$ , we say that there exists interaction between the coordinate directions  $t_p$  and  $t_q$  and covariance functions of the form (3) become nonseparable. Large values of  $\sigma_\varepsilon^2$  and of  $b_q$  both result in more fluctuation of  $X$  over  $\mathbf{t}$ . The estimated values of these two hyperparameters, however, indicate whether the fluctuation of  $X$  over  $\mathbf{t}$  is explained by the signal  $f$  or by the noise  $\varepsilon$ .

The specification of the covariance function is important because it fixes the properties (e.g. stationarity, separability) of the underlying function  $f$  that we want to infer. Several families of stationary covariance functions can be chosen, such as the powered exponential, rational quadratic, and Matérn families (Shi and Choi, 2011). Each family has adjustable parameters which allows separate effects for each coordinate in  $\mathbf{t}$  and can be inferred from the data. Selection of covariance functions is discussed in Rasmussen and Williams (2006) and Shi and Choi (2011).

When  $\mathbf{t}$  is multi-dimensional, a general nonparametric covariance cannot usually be used due to the curse of dimensionality. One way to address the problem is to assume a separable covariance function

$$k(\mathbf{t}, \mathbf{t}') = k_1(t_1, t'_1) \cdots k_Q(t_Q, t'_Q), \quad (4)$$

that is, if it can be factorised into the product between covariance functions, each one corresponding to one dimension, then it can be modelled nonparametrically (see e.g. Chen et al., 2017; Rougier, 2017).

In this paper, we propose a semiparametric approach for the estimation of a flexible covariance function in such way we can relax the assumptions of stationarity and separability. The nonstationarity over  $\mathbf{t}$  is defined by a convolution-based approach via a varying kernel, whose parameters are modelled nonparametrically. In particular, we propose to use a suitable parametrisation for the varying anisotropy matrix, allowing unconstrained estimation.

## 2.2 Nonstationary covariance functions

The linear covariance function  $k(\mathbf{t}, \mathbf{t}') = \sum_{q=1}^Q a_q \mathbf{t}_q \mathbf{t}'_q$  (Shi and Choi, 2011) is an example of nonstationary covariance function. Its simplicity, though, is of limited use for modelling complex covariance structures and it is often used together with other covariance functions (e.g. Wang and Shi (2014)).

A popular strategy to deal with nonstationarity in spatial statistics literature is through *deformation* (Sampson and Guttorp, 1992). The idea is to transform the geographical space into another space where stationarity holds. The choice of a suitable transformation is a challenging task. In addition, this approach requires independent replications of the spatial process.

Higdon et al. (1999) propose a constructive, convolution-based approach to account for nonstationarity in the covariance function. A spatial process  $f(\cdot)$  is represented as the convolution of a Gaussian white noise process  $z(\cdot)$  with a kernel  $k_{\mathbf{t}}$ , that is,

$$f(\mathbf{t}) = \int_{\mathbb{R}^Q} k_{\mathbf{t}}(\mathbf{u})z(\mathbf{u})d\mathbf{u}, \quad (5)$$

where the nonstationarity is achieved by considering a spatially-varying kernel  $k_{\mathbf{t}}$ . The covariance function of (5) takes the form

$$\text{Cov}[f(\mathbf{t}), f(\mathbf{t}')] = \int_{\mathbb{R}^Q} k_{\mathbf{t}}(\mathbf{u})k_{\mathbf{t}'}(\mathbf{u})d\mathbf{u} \quad (6)$$

and is positive definite provided that  $\sup \int_{\mathbb{R}^Q} k_{\mathbf{t}}(\mathbf{u})^2 d\mathbf{u} < \infty$ .

The convolution-based approach has become popular mainly because specifying a kernel which satisfies the above condition is much easier than a covariance function directly. Higdon (2002) suggests different process convolution specifications to build flexible space and space-time models.

Paciorek and Schervish (2006) show that the covariance function (6) is valid in every Euclidean space  $\mathbb{R}^Q$ ,  $Q = 1, 2, \dots$ . They also note that if we assume a Gaussian kernel  $k_{\mathbf{t}}(\mathbf{u}) = (2\pi)^{-Q/2} |\Sigma|^{-1/2} \exp\{- (1/2)(\mathbf{t} - \mathbf{u})^T \Sigma(\mathbf{t})^{-1}(\mathbf{t} - \mathbf{u})\}$ , the covariance function of  $f(\cdot)$  will be

$$\text{Cov}[f(\mathbf{t}), f(\mathbf{t}')] = \sigma^2 |\Sigma(\mathbf{t})|^{1/4} |\Sigma(\mathbf{t}')|^{1/4} \left| \frac{\Sigma(\mathbf{t}) + \Sigma(\mathbf{t}')}{2} \right|^{-1/2} \exp\{-Q_{\mathbf{t}\mathbf{t}'}\}, \quad (7)$$

where

$$Q_{\mathbf{t}\mathbf{t}'} = (\mathbf{t} - \mathbf{t}')^T \left( \frac{\Sigma(\mathbf{t}) + \Sigma(\mathbf{t}')}{2} \right)^{-1} (\mathbf{t} - \mathbf{t}').$$

A more general class for nonstationary covariance functions given by

$$\text{Cov}[f(\mathbf{t}), f(\mathbf{t}')] = \sigma(\mathbf{t})\sigma(\mathbf{t}')|\Sigma(\mathbf{t})|^{1/4}|\Sigma(\mathbf{t}')|^{1/4}\left|\frac{\Sigma(\mathbf{t}) + \Sigma(\mathbf{t}')}{2}\right|^{-1/2}g\left(\sqrt{Q_{\mathbf{t}\mathbf{t}'}}\right), \quad (8)$$

where  $g(\cdot)$  is a valid isotropic correlation function.

Even if the anisotropy matrix is assumed to be constant ( $\Sigma(\mathbf{t}) = \Sigma$ ), the covariance function (8) is also nonstationary. In this special case, the nonstationarity is introduced through scaling of a stationary process (Banerjee et al., 2015, Section 3.2). In other words, if a stationary process  $V(\mathbf{t})$  has mean 0, variance 1 and correlation function  $\rho$ , then  $Z(\mathbf{t}) = \sigma(\mathbf{t})V(\mathbf{t})$  is a nonstationary process with covariance function  $\text{Cov}[Z(\mathbf{t}), Z(\mathbf{t}')] = \sigma(\mathbf{t})\sigma(\mathbf{t}')\rho(\mathbf{t} - \mathbf{t}')$ . The composite Gaussian process model (Ba and Joseph, 2012) also uses this idea to allow varying volatility.

The anisotropy matrix  $\Sigma(\mathbf{t})$ , though, measures how quickly varying is the fluctuation of the random processes over  $\mathbf{t}$  and one may want to allow it to vary over  $\mathbf{t}$ . Both  $\sigma(\cdot)$  and  $\Sigma(\cdot)$  can also vary over  $\boldsymbol{\tau} \in \mathcal{T}^* \subset \mathbb{R}^{Q^*}$ , where  $Q^* \leq Q$ . This  $\boldsymbol{\tau}$  can represent, for example, time or spatial coordinates, accounting for time-varying or spatially-varying parameters, or both. This provides a flexible way to model nonstationary and nonseparable covariance structure. We will use the observed data to estimate the covariance structure nonparametrically. The details will be discussed in the next subsection.

If  $g$  is, for example, a (squared) exponential function, it is easy to see that if and only if we can factorise  $\sigma(\mathbf{t}) = \sigma(t_1) \cdots \sigma(t_Q)$  and have zero off-diagonal elements in  $\Sigma(\mathbf{t})$ , then a separable covariance function (4) is obtained.

### 2.2.1 Parametrisation of the varying anisotropy matrix

We must ensure positive definiteness of the anisotropy matrix  $\Sigma(\mathbf{t})$  in (8). This can be done by using different parametrisations. For example, Higdon (1998); Higdon et al. (1999); Risser and Calder (2017) use geometrically-based parametrisations which capture local anisotropy by rotating and stretching coordinate directions. Paciorek and Schervish (2006) suggest using a spectral decomposition. However, these methods are either designed for some special cases or are difficult to form interpretation about its elements.

Pinheiro and Bates (1996) present other five parametrisations for a covariance matrix, one of which is the spherical parametrisation, a particularly interesting strategy because it provides direct interpretation of parameters in terms of variances and correlations. We propose using the spherical parametrisation for  $\Sigma(\mathbf{t})$  and interpret the parameters in terms of length-scale (to assess how rapidly varying is the function  $f$  of eq. (1) in each coordinate direction) and direction of dependence (to see potentially interaction between the coordinate directions).

As discussed above, the off-diagonal elements of  $\Sigma(\mathbf{t})$  have to be zero to produce a separable covariance function. Therefore, a value which is distant from zero indicates nonseparable covariance structure due to the interaction between the coordinate directions of  $\mathbf{t}$  in the way the process fluctuates over  $\mathbf{t}$ .

We will consider the Cholesky decomposition

$$\Sigma(\mathbf{t}) = \Sigma(\boldsymbol{\tau}) = \mathbf{L}(\boldsymbol{\tau})^\top \mathbf{L}(\boldsymbol{\tau}),$$

where  $\mathbf{L}$  is an  $Q \times Q$  upper triangular matrix (including the main diagonal). Positiveness of the main diagonal entries of  $\mathbf{L}$  ensures that  $\Sigma$  is positive definite.

We will follow closely the exposition of Pinheiro and Bates (1996) to explain the spherical parametrisation. Let  $\mathbf{L}_q$  denote the  $q$ -th column of  $\mathbf{L}$  and  $\ell_q$  denote the spherical coordinates of the first  $q$  elements of  $\mathbf{L}_q$ . Therefore, we have

$$\begin{aligned} [L_q]_1 &= [\ell_q]_1 \cos([\ell_q]_2), \\ [L_q]_2 &= [\ell_q]_1 \sin([\ell_q]_2) \cos([\ell_q]_3), \\ &\dots, \\ [L_q]_{q-1} &= [\ell_q]_1 \sin([\ell_q]_2) \cdots \cos([\ell_q]_q), \\ [L_q]_q &= [\ell_q]_1 \sin([\ell_q]_2) \cdots \sin([\ell_q]_q). \end{aligned}$$

Let us define a diagonal matrix  $\mathbf{C}$  whose diagonal entries are  $[\mathbf{C}_{qq}] = [\Sigma_{qq}]^{1/2}$ . Then we can write  $\Sigma$  in terms of a matrix  $\mathbf{R}$

$$\Sigma = \mathbf{C}^{1/2} \mathbf{R} \mathbf{C}^{1/2},$$

where  $\mathbf{R}_{qq} = 1$ ,  $q = 1, \dots, Q$ , and  $\mathbf{R}_{pq} = \rho_{pq}$ ,  $p \neq q$ . The parameter  $\rho_{pq} \in (-1, 1)$  measures the direction of linear dependence between the coordinates  $p$  and  $q$ . If  $\rho_{pq} \neq 0$  for some pair  $(p, q)$ , then the covariance function (8) is nonseparable. The value of  $\Sigma_{qq}$  can be interpreted as the length-scale parameter and therefore measures how rapidly varying is the function  $f$  in (1) towards the coordinate  $q$ .

We can show that  $\Sigma_{qq} = [\ell_q]_1^2$  and that  $\rho_{1q} = \cos([\ell_q]_2)$ ,  $q = 2, \dots, Q$ , with  $-1 < \rho_{1q} < 1$ . This means that we can interpret the values of  $\mathbf{L}$  in terms of the length-scale parameters and directions of dependence of  $\Sigma$ .

The spherical parametrisation is unique if

$$\begin{aligned} [\ell_q]_1 &> 0, \quad q = 1, \dots, Q, \\ [\ell_q]_p &\in (0, \pi), \quad q = 2, \dots, Q, \quad p = 2, \dots, q. \end{aligned}$$

We can then easily proceed with an unconstrained estimation by defining a new vector of parameters  $\alpha$  including  $\log([\ell_q]_1)$ ,  $q = 1, \dots, Q$ , and  $\log([\ell_q]_p / (\pi - [\ell_q]_p))$ ,  $q = 2, \dots, Q$ ,  $p = 2, \dots, q$ . The upper triangular matrix  $\mathbf{L}$  can be reparametrised by  $\alpha$ . Each element  $\alpha_j = \alpha_j(\tau)$ , for  $j = 1, \dots, Q(Q+1)/2$ , depends on  $\tau$  if the covariance structure is nonstationary.

The unconstrained estimation of each element of  $\alpha$  allows it to be modelled as a nonparametric function of  $\tau$ . The spherical parametrisation has some other advantages over other parametrisations in that: (i) it is uniquely defined and can be readily extended for any  $Q > 2$ , which is difficult when implementing geometrically-based parametrisations; (ii) it has about the same computational efficiency as the Cholesky parametrisation applied directly; (iii) it has less parameters to be estimated than the spectral decomposition; (iv) we can make interpretations for the elements of  $\mathbf{L}$ ; and (v) we can account for uncertainty on  $\alpha$ , and consequently conduct inference on length-scale and direction of dependence.

A geometrical interpretation of the spherical parametrisation can be seen in Rapisarda et al. (2007). Other parametrisations based on Cholesky decomposition has been widely discussed.

Zhang et al. (2015) mention that unconstrained nature of the parametrisation of the Cholesky factor allows to represent angles of the spherical parametrisation via regression as functions of some covariates, an idea also used by Pourahmadi (1999) and Leng et al. (2010) when parametrising covariance matrices using a modified Cholesky decomposition.

If the covariance structure depends along one coordinate direction  $\tau \subset \mathbb{R}$  (i.e.  $Q^* = 1$ , e.g. time-varying parameters), many nonparametric methods can be used, e.g.

$$\alpha_j(\tau) = \sum_{l=1}^L \theta_{jl} B_{jl}(\tau), \quad (9)$$

where  $B_\ell$  form B-spline basis functions (de Boor, 2001). This representation ensures that the resulting function is smooth but still very flexible as we can change the degree of the piecewise polynomials and the number and location of knots. The locations of the knots are usually the quantiles of  $\tau$ , but they can be chosen differently; we can also allow discontinuities in derivatives by repeating knots at the same location. The gain of adding more knots comes with the cost of increasing the number of parameters to be estimated. Typically, the number of knots is chosen by cross-validation. Some other methods can be used, e.g. Ba and Joseph (2012) use a Gaussian kernel regression model.

For multidimensional  $\tau \subset \mathbb{R}^{Q^*}$  (useful to model spatially-varying parameters), we can construct multivariate B-splines basis function by taking the product of the  $Q^*$  univariate basis.

An alternative method is to use a Gaussian process to model each  $\alpha_j(\tau)$  using a parametric covariance function. Let  $\alpha_{ji} = \alpha_j(\tau_i)$ ,  $i = 1, \dots, n$ . Then we define

$$(\alpha_{j1}, \dots, \alpha_{jn}) \sim N(\mathbf{0}, \mathbf{K}_j(\theta_j)), \quad (10)$$

where  $\mathbf{K}_j$  is an  $n \times n$  covariance matrix where its  $(i, i')$ -th element is calculated by the covariance function  $k_j(\tau_i, \tau_{i'}; \theta_j)$ , depending on unknown parameter  $\theta_j$ . In practice, we may use the same covariance function for  $j = 1, \dots, Q$  and for  $j = Q + 1, \dots, Q(Q + 1)/2$ . This method can cope with the large dimensional cases, i.e.  $Q^* > 1$ .

### 2.2.2 Model learning

We now denote the covariance function constructed by (8) and the above parametrisation methods by  $k(\mathbf{t}, \mathbf{t}'; \theta)$  for any  $\mathbf{t}, \mathbf{t}' \in \mathbb{R}^Q$ , where  $\theta$  includes all the unknown parameters in (9) if B-splines are used or in (10) if GPRs are used; in addition,  $\theta$  includes  $\log(\sigma^2)$  in (7). We will use an empirical Bayesian approach to estimate the unknown parameters and thus the nonstationary covariance structure.

For a given set of observed data  $\mathcal{D} = \{\mathbf{x}, \mathbf{t}\} = \{(x_i, t_{i1}, \dots, t_{iQ}), 1, \dots, n\}$ , a GPR model for (1) can be written as

$$\begin{aligned} x_i | f_i &\stackrel{\text{i.i.d.}}{\sim} N(f_i, \sigma_\varepsilon^2), \\ (f_1, \dots, f_n) &\sim GP(\mathbf{0}, k(\cdot, \cdot; \theta)), \end{aligned} \quad (11)$$



where the covariance function  $k(\cdot, \cdot; \boldsymbol{\theta})$  may be nonstationary, constructed using the methods discussed above. Thus, the marginal distribution of  $\mathbf{x}$  given  $\boldsymbol{\theta}$  is

$$p(\mathbf{x}|\boldsymbol{\theta}) = \int p(\mathbf{x}|\mathbf{f})p(\mathbf{f}|\boldsymbol{\theta})d\mathbf{f},$$

where  $p(\mathbf{x}|\mathbf{f}) = \prod_{i=1}^n \zeta(f_i)$ , with  $\zeta(f_i)$  denoting the normal probability density function with mean  $f_i$  and variance  $\sigma_\varepsilon^2$ , and  $\mathbf{f} = (f(t_1), \dots, f(t_n))^\top \sim N(\mathbf{0}, \mathbf{K}_n)$ , where  $[\mathbf{K}_n]_{ij} = k(\mathbf{t}_i, \mathbf{t}_j)$ ,  $i, j = 1, \dots, n$ . For convenience,  $\boldsymbol{\theta}$  includes the parameter  $\sigma_\varepsilon^2$  as well. For Gaussian data defined in (11), the marginal distribution of  $\mathbf{x}$  is  $N(\mathbf{0}, \boldsymbol{\Psi}_n)$ , where  $\boldsymbol{\Psi}_n = \mathbf{K}_n + \sigma_\varepsilon^2 \mathbf{I}_n$ , the marginal log-likelihood of  $\boldsymbol{\theta}$  is given by

$$\mathcal{L}(\boldsymbol{\theta}|\mathcal{D}) = -\frac{1}{2} \log |\boldsymbol{\Psi}_n(\boldsymbol{\theta})| - \frac{1}{2} \mathbf{x}' \boldsymbol{\Psi}_n(\boldsymbol{\theta})^{-1} \mathbf{x} - \frac{n}{2} \log 2\pi. \quad (12)$$

The estimates of  $\boldsymbol{\theta}$  in (12) are called empirical Bayes estimates as they are obtained by using observed data (Carlin and Louis, 2008).

To reduce the computational costs when calculating the determinant and the inverse of  $\boldsymbol{\Psi}_n$  in (12), we can instead use the local likelihood estimation (LLE) (Tibshirani and Hastie, 1987). In the LLE, instead of maximising (12) directly, we maximise

$$\mathcal{L}_k(\boldsymbol{\theta}_k|\mathcal{D}_k) = -\frac{1}{2} \log |\boldsymbol{\Psi}(\boldsymbol{\theta}_k)| - \frac{1}{2} \mathbf{x}'_k \boldsymbol{\Psi}(\boldsymbol{\theta}_k)^{-1} \mathbf{x}_k - \frac{n_k}{2} \log 2\pi \quad (13)$$

locally, where  $k$  is the index of location  $\mathbf{t}_k$ . Estimates of  $\boldsymbol{\theta}_k$  are obtained by considering only the data in the neighbourhood of  $\mathbf{t}_k$ , that is,  $\mathcal{D}_k = \{(\mathbf{x}_i, \mathbf{t}_i) : \|\mathbf{t}_i - \mathbf{t}_k\| < r\}$ , where  $r$  is a predefined radius. Using the available observations in the neighbourhood of  $\mathbf{t}_k$  is important as the behaviour of the covariance function near the origin determines properties of the process (Stein, 1999). Risser and Calder (2017) suggest a mixture component approach in which they estimate the spatially varying parameters  $\boldsymbol{\theta}_k$ ,  $k = 1, \dots, k_{max}$ , locally and then, for any arbitrary location  $\mathbf{t}$ ,  $\boldsymbol{\theta}_k(\mathbf{t})$  is obtained by averaging, respectively,  $\boldsymbol{\theta}_k$ ,  $k = 1, \dots, k_{max}$ , with a weight function depending on the distance between  $\mathbf{t}_k$  and  $\mathbf{t}$ .

A special case is when the nonstationarity depends on one coordinate direction as discussed around equation (9). We can use B-spline basis functions and then estimate the corresponding coefficients  $\theta_{jl}$ . In practice, we may simply estimate  $\boldsymbol{\theta}_j$  locally for some locations via (13) (i.e. assuming  $\boldsymbol{\theta}_j$  is a constant in a neighbourhood of the locations) and then regress these estimates to obtain smooth functions  $\boldsymbol{\theta}_j(\boldsymbol{\tau})$  for any  $\boldsymbol{\tau} \in \mathbb{R}^{Q^*}$ , using a nonparametric approach, e.g. B-splines.

## 3 Prediction and decomposition of function-valued processes

### 3.1 Bayesian prediction and decomposition

Let us consider the GPR model (11). The posterior distribution  $p(\mathbf{f}|\mathcal{D}, \sigma_\varepsilon^2)$  is a multivariate Gaussian distribution with  $E[\mathbf{f}|\mathcal{D}, \sigma_\varepsilon^2] = \mathbf{K}_n(\mathbf{K}_n + \sigma_\varepsilon^2 \mathbf{I}_n)^{-1} \mathbf{x}$  and  $\text{Var}[\mathbf{f}|\mathcal{D}, \sigma_\varepsilon^2] = \sigma_\varepsilon^2 \mathbf{K}_n(\mathbf{K}_n + \sigma_\varepsilon^2 \mathbf{I}_n)^{-1}$ .

The marginal distribution of  $\mathbf{x}$  is  $N(\mathbf{0}, \Psi_n)$ , where  $\Psi_n = \mathbf{K}_n + \sigma_\varepsilon^2 \mathbf{I}_n$ . Therefore, we can easily make predictions of test data at locations  $\mathbf{t}$  given the observed data  $\mathcal{D}$ . The posterior distribution  $p(f(\mathbf{t})|\mathcal{D})$  also has multivariate normal distribution with

$$\begin{aligned} E[f(\mathbf{t})|\mathcal{D}] &= \mathbf{k}_n^\top(\mathbf{t})(\mathbf{K}_n + \sigma_\varepsilon^2 \mathbf{I}_n)^{-1} \mathbf{x}, \\ \text{Var}[f(\mathbf{t})|\mathcal{D}] &= k(\mathbf{t}, \mathbf{t}) - \mathbf{k}_n^\top(\mathbf{t})(\mathbf{K}_n + \sigma_\varepsilon^2 \mathbf{I}_n)^{-1} \mathbf{k}_n(\mathbf{t}), \end{aligned} \quad (14)$$

where  $\mathbf{x} = (x(\mathbf{t}_1), \dots, x(\mathbf{t}_n))^\top$ ,  $\mathbf{K}_n = (k(\mathbf{t}_i, \mathbf{t}_j))_{n \times n}$ ,  $\mathbf{k}_n(\mathbf{t}) = (k(\mathbf{t}_1, \mathbf{t}), \dots, k(\mathbf{t}_n, \mathbf{t}))^\top$ .

However, the predictive distribution becomes much more complicated for non-Gaussian data (see e.g. Wang and Shi (2014)). We may therefore consider using the decomposition methods detailed below.

Once estimated the covariance function  $k(\cdot, \cdot)$ , we can estimate the corresponding eigenfunctions  $\phi(\cdot)$  via Nyström method for approximating eigenfunctions. Then a finite GPR approximation can be obtained as in (15) by using only the first  $J$  eigenfunctions. This allows us to make predictions at any arbitrary location  $\mathbf{t}$  given observed data  $\mathbf{x}$  and a finite number of components  $\phi(\cdot)$  similarly as in FPCA:

$$X(\mathbf{t}) = \mu(\mathbf{t}) + \sum_{j=1}^{\infty} \xi_j \phi_j(\mathbf{t}), \quad (15)$$

where  $\mu$  is the mean function and  $\xi_j$  are uncorrelated random variables and  $\phi_j$  are eigenfunctions of the covariance operator of  $X$  (Karhunen-Loève expansion), i.e.  $\phi_j$  are solutions to the equation

$$\int k(\mathbf{t}, \mathbf{t}') \phi(\mathbf{t}') d\mathbf{t}' = \lambda \phi(\mathbf{t}).$$

The decomposition (15) is especially useful to identify the main modes of variation in the data. In addition, the covariance function  $k(\cdot, \cdot)$  is  $(2 \times Q)$ -dimensional, which makes its visualisation rather difficult; therefore, it might be important to look at its eigenfunctions to identify some of features of the covariance function.

The eigenvalue  $\lambda_j$  is the variance of  $X$  in the principal direction  $\phi_j$  and the cumulative fraction of variance explained by the first  $J$  directions is given by

$$\text{CFVE}_J = \frac{\sum_{j=1}^J \lambda_j}{\sum_{j=1}^M \lambda_j}, \quad \text{where } M \text{ is large.} \quad (16)$$

Note that the decomposition (15) is based on the covariance function  $k(\mathbf{t}, \mathbf{t}')$ ,  $\mathbf{t}, \mathbf{t}' \in \mathbb{R}^Q$ , constructed and learned by the methods discussed in the previous section. It can model the covariance structure even if it is nonstationary or nonseparable. By contrast, most of the existing methods are based on the separable assumptions for the multidimensional case, (i.e.  $Q > 1$ ). For example, Chen et al. (2017) suggest using tensor product representations. In the model that they called Product FPCA, the two-dimensional function-valued process  $X$  is represented as

$$X(s, \tau) = \mu(s, \tau) + \sum_{j=1}^{\infty} \sum_{l=1}^{\infty} \chi_{jl} \phi_j(s) \psi_l(\tau),$$

where  $\phi$  and  $\psi$  are the eigenfunctions of the marginal covariance functions for the  $Q = 2$ -dimensional case.

## 3.2 Asymptotic theory

In this subsection, we provide asymptotic theory for the decomposition and Bayesian prediction based on a Gaussian process prior with a general covariance structure discussed above.

In eq. (15),  $\xi_j$  are independent normal random variables and  $\phi_j(\cdot)$  are the eigenfunctions of the kernel function  $k(\cdot, \cdot)$ . Therefore, the eigenfunctions are orthonormal satisfying

$$\int k(\mathbf{t}, \mathbf{t}') \phi_j(\mathbf{t}) d\mathbf{t} = \lambda_j \phi_j(\mathbf{t}), \quad \int \phi_i(\mathbf{t}) \phi_j(\mathbf{t}) d\mathbf{t} = \delta_{ij},$$

where  $\lambda_1 \geq \lambda_2 \geq \dots \geq 0$  are the eigenvalues of  $k(\cdot, \cdot)$  and  $\delta_{ij}$  is the Kronecker delta.

Let  $X^c(\mathbf{t}) = X(\mathbf{t}) - \mu(\mathbf{t})$  and  $\Phi(f) = \int_{\mathcal{T}} k(\mathbf{t}, \cdot) f(\mathbf{t}) d\mathbf{t}$  be an operator for  $f \in L^2(\mathcal{T})$ . In fact,

$$\xi_j = \langle X^c(\cdot), \phi_j(\cdot) \rangle = \int X^c(\mathbf{t}) \phi_j(\mathbf{t}) d\mathbf{t}$$

has mean 0 and variance  $\lambda_j$ .

**Theorem 1.** *For  $J \geq 1$ , for which  $\lambda_J > 0$ , the functions  $\{\phi_j, j = 1, \dots, J\}$  provide the best finite dimensional approximation to  $X^c(\mathbf{t})$  with respect to minimising criterion*

$$\operatorname{argmin}_{g_1, \dots, g_J \in L^2(\mathcal{T})} E \left[ \left\| X^c(\mathbf{t}) - \sum_{j=1}^J g_j(\mathbf{t}) \xi_j^* \right\|^2 \right], \quad (17)$$

where  $g_1, \dots, g_J \in L^2(\mathcal{T})$  are orthonormal and  $\xi_j^* = \langle X^c(\cdot), g_j(\cdot) \rangle = \int X^c(\mathbf{t}) g_j(\mathbf{t}) d\mathbf{t}$ . The minimising value is  $\sum_{j=J+1}^{\infty} \lambda_j$ .

The proof is given in Appendix A.1. This theorem is similar to Theorem 1 in Chen et al. (2017); but the latter provides the best finite approximation under separability assumption. The above theorem is true for a very general covariance structure even if it is nonstationary or nonseparable.

The following theorem provides the convergence rates also under a general covariance structure.

**Theorem 2.** *Suppose conditions C1 - C3 in Appendix hold, and  $\hat{\mu}(\mathbf{t})$  satisfies  $\sup_{\mathbf{t}} |\hat{\mu}(\mathbf{t}) - \mu(\mathbf{t})| = O_p(\{\log(n)/n\}^{1/2})$ , we have, for  $1 \leq j \leq J$ ,*

$$\begin{aligned} \|k_{\hat{\theta}}(\cdot, \cdot) - k_{\theta}(\cdot, \cdot)\| &= O_p(\{\log(n)/n\}^{1/2}), \\ \|\hat{\lambda}_j - \lambda_j\| &= O_p(\{\log(n)/n\}^{1/2}), \\ \|\hat{\phi}_j(\cdot) - \phi_j(\cdot)\| &= O_p(\{\log(n)/n\}^{1/2}), \\ \|\hat{\xi}_j - \xi_j\| &= O_p(\{\log(n)/n\}^{1/2}). \end{aligned}$$

The proof is given in Appendix A.2.

We now look at the relationship between the Bayesian prediction and the decomposition based on Karhunen-Loève expansion. Using models (1) and (2), where  $f \sim GP(0, k)$  with  $k = k_{\theta}$  and  $\varepsilon(\mathbf{t})$  is a Gaussian error process  $GP(0, k_{\varepsilon})$  with  $k_{\varepsilon}(\mathbf{t}, \mathbf{t}') = \sigma_{\varepsilon}^2 I(\mathbf{t} = \mathbf{t}')$ . Hence,  $X \sim GP(0, \tilde{k}_{\theta})$  with  $\tilde{k}_{\theta} = k_{\theta} + k_{\varepsilon}$ . Given  $\mathbf{f} = (f(\mathbf{t}_1), \dots, f(\mathbf{t}_n))^{\top}$ , we use  $E[f(\mathbf{t})|\mathbf{f}] = \mathbf{k}_n^{\top}(\mathbf{t}) \mathbf{K}_n^{-1} \mathbf{f}$  to estimate  $f(\mathbf{t})$ . Given the observed data  $\mathcal{D}$ , we use (14) to estimate  $f(\mathbf{t})$ .

In addition, from Karhunen-Loève expansion we have

$$f(\mathbf{t}) = \sum_{j=1}^{\infty} \phi_j(\mathbf{t})\xi_j, \quad X(\mathbf{t}) = \sum_{j=1}^{\infty} \tilde{\phi}_j(\mathbf{t})\tilde{\xi}_j, \quad (18)$$

where  $\phi_j(\cdot)$  and  $\tilde{\phi}_j(\cdot)$  are the eigenfunctions of  $k_\theta$  and  $\tilde{k}_\theta$ , respectively, and their corresponding eigenvalues are  $\lambda_1 \geq \lambda_2 \geq \dots \geq 0$  and  $\tilde{\lambda}_1 \geq \tilde{\lambda}_2 \geq \dots \geq 0$ , respectively. The truncated sum of (18) will be

$$f_n(\mathbf{t}) = \sum_{j=1}^n \phi_j(\mathbf{t})\xi_j, \quad X_n(\mathbf{t}) = \sum_{j=1}^n \tilde{\phi}_j(\mathbf{t})\tilde{\xi}_j.$$

**Theorem 3** *Under conditions in Theorem 2, we have  $E[f(\mathbf{t})|\mathbf{f}] = f_n(\mathbf{t}) + o_p(1)$ . Moreover, under model (1),  $E[f(\mathbf{t})|\mathcal{D}] = X_n(\mathbf{t}) + o_p(1)$ .*

The proof is given in Appendix A.3. This theorem indicates that the Bayesian prediction and Karhunen-Loève expansion provide similar results. This gives flexibility in functional data analysis. If we are mainly interested in a predictive model for Gaussian data, we may just use the Bayesian prediction. The implementation is fairly efficient if the sample size is not very large. However, if we are also interested in how the covariance is structured, we may study the eigenfunctions and the eigenvalues; more discussion will be given in the next two sections. This also provides a way to develop efficient approximation for big data (e.g. Nyström method (Shi and Choi, 2011, p.42)) or for non-Gaussian data.

## 4 Simulation studies

In this section, we show two examples of data with nonseparable, nonstationary covariance structure. We also discuss how directions of linear dependence between coordinates can be visualised and show that nonseparable models can explain more variation in the data using less components. An additional simulation study can be seen in Appendix A.4.

### 4.1 Simulation study 1

In this study, we simulate a three-dimensional function-valued process  $X(\tau, s_1, s_2)$ , where  $\tau, s_1, s_2 \in [0, 1]$ , from (1), where  $f$  is zero-mean  $T$ -process with covariance function (8) and squared exponential correlation kernel  $g(\cdot)$ . We also set  $\sigma_\varepsilon^2 = 0.1$ . We assume that the parameters  $\sigma^2$  and  $\Sigma$  in (8) depend only on  $\tau$ . This example is comparable to spatiotemporal models which have time and spatial coordinates as input variables and time-varying coefficients (e.g. dynamic linear models (Banerjee et al., 2015)).

We set  $\sigma^2(\tau) = \exp(\tau)$  and

$$\Sigma(\tau) = \begin{bmatrix} 1 & 0 & 0 \\ 0 & 1 & \rho_{23}(\tau) \\ 0 & \rho_{23}(\tau) & 1 \end{bmatrix},$$

with  $\rho_{23}(\tau) = 0.95 \tau$ . That is, the process  $f$  has overall variance  $\sigma^2(\cdot)$  and the interaction between coordinate directions  $s_1$  and  $s_2$ , given by  $\rho_{23}(\cdot)$ , increases over  $\tau$ . This produces a nonstationary, nonseparable covariance function.

As  $\tau$  increases,  $\rho_{23}$  becomes more distant from zero, and thus models which assume separable covariance structure might be not suitable. Figs 1 and 2, show, for  $\tau = 0.25$  and  $\tau = 1$ , respectively, the true leading eigensurfaces  $\phi(\tau, s_1, s_2)$  and the corresponding estimates obtained by nonstationary GP (NSGP) and Product FPCA.

The first eigensurface represents the direction of the largest variation in the data relative to the mean function. The second eigensurface corresponds to the direction of the largest variation which is orthogonal to the first eigensurface, and so forth. Covariance separability implies separability of eigensurfaces. Therefore, if we observe nonseparable eigensurfaces, this means that the separability assumption is not satisfied.

Although the data were simulated from a  $T$ -process, the NSGP model obtains estimated eigensurfaces quite similar to the true ones. The model clearly identifies that the interaction between  $s_1$  and  $s_2$  becomes stronger for higher values of  $\tau$  – see how the diagonal orientation is clearer as  $\tau$  increases from Fig. 1 to Fig. 2. This fact is not detected by the Product FPCA model as this assumes separability of the eigensurfaces.

In practice, one eigensurface can often be interpreted as a *size* component; if the corresponding contour plot is ellipsoidal with diagonal orientation, then a model which assumes separability will not describe it well. The visualisation of eigensurfaces can also identify, for example, a contrast between low-latitude and high-latitude; this contrast, however, might not be constant over longitude. If we allow for nonseparability, we can identify, for example, a contrast between between northwest and southeast (see e.g. the second true eigensurface in Fig. 2, assuming that  $s_1$  and  $s_2$  represent longitude and latitude, respectively).

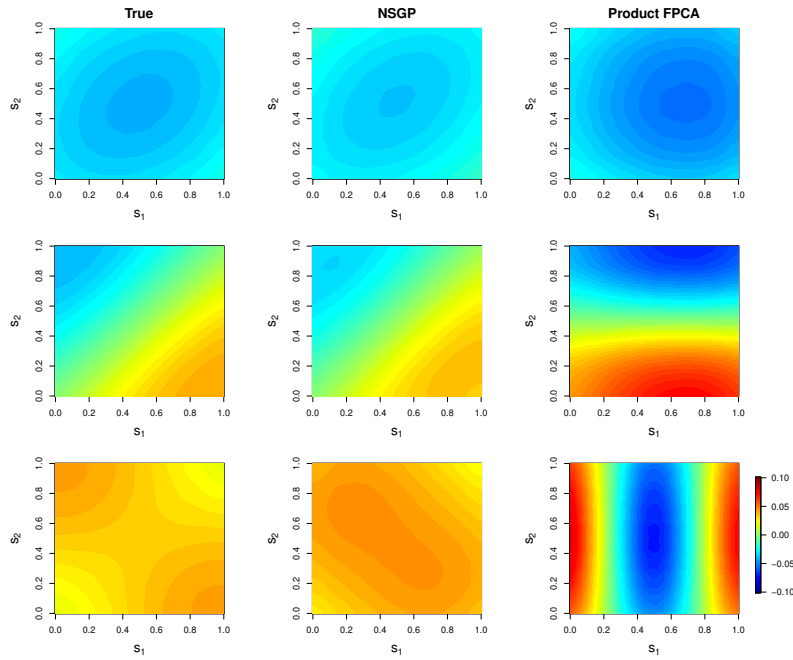


**Fig. 1.** First four leading eigensurfaces  $\phi(0.25, s_1, s_2)$  of the true model (left column) and the corresponding estimated eigensurfaces  $\hat{\phi}(0.5, s_1, s_2)$  from the NSGP model (centre) and Product FPCA model (right).

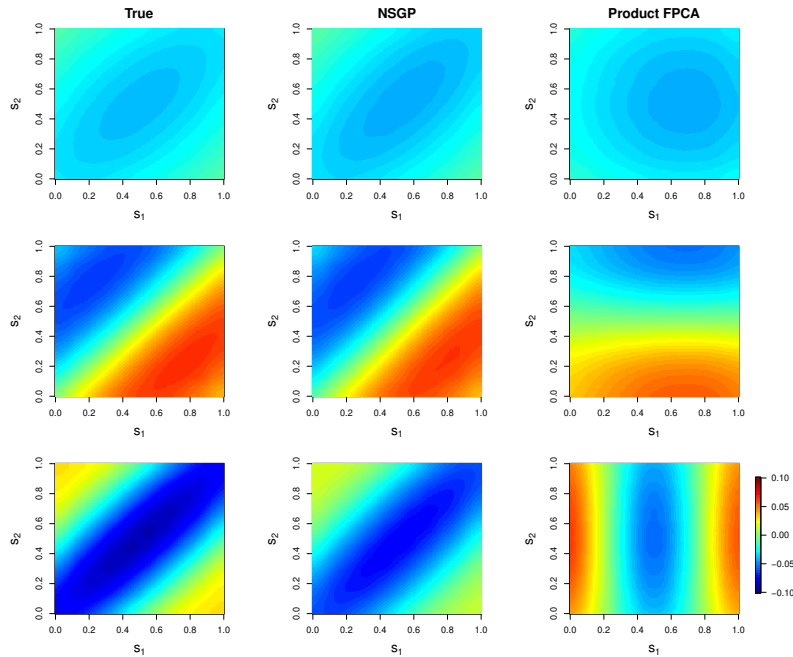


**Fig. 2.** First four leading eigensurfaces  $\phi(1, s_1, s_2)$  of the true model (left column) and the corresponding estimated eigensurfaces  $\hat{\phi}(1, s_1, s_2)$  from the NSGP model (centre) and Product FPCA model (right).

The CFVEs calculated by (16) for the first 16 leading three-dimensional eigensurfaces and are illustrated in Fig. 3. As expected, the advantage of the nonseparable model in terms of CFVE is clear not in the first, but in later components. In addition, we can conclude that the NSGP model requires less components to explain the same amount of variation in this dataset.

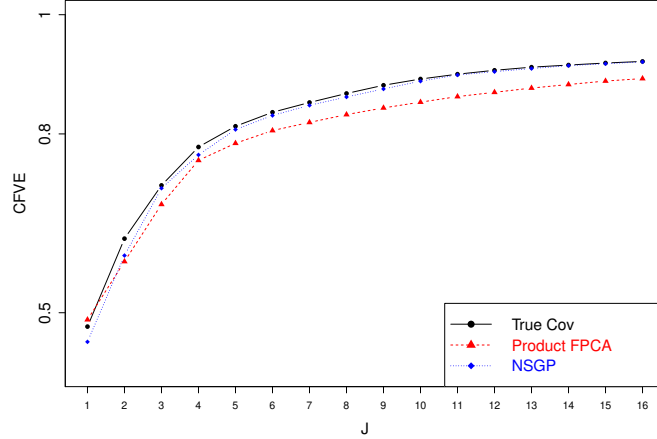


**Fig. 3.** Comparison of cumulative FVEs obtained by the true, and Product FPCA, and NSGP models.

## 4.2 Simulation study 2

In this simulation study, we assume that the two-dimensional function-valued process  $X(s_1, s_2)$  has zero mean function and covariance function given by  $\text{Cov}[X(\mathbf{s}), X(\mathbf{s}')] = \sum_{j=1}^{20} \alpha_j \phi_j(s_1 + s_2) \phi_j(s'_1 + s'_2)$ , where  $\phi_j(\cdot)$  are Chebyshev polynomials,  $\alpha_j = j^{-3/2}$  and  $\mathbf{s} \in [-1, 1]^2$ . The basis functions of the form  $\phi_j(s_1 + s_2)$  are clearly nonseparable and produce a nonseparable covariance structure.

We generate 100 surfaces observed at  $n_1 \times n_2 = 20 \times 20 = 400$  equally spaced points and estimated the covariance structure by the NSGP and Product FPCA models. Fig. 4 illustrates that the NSGP model obtains more accurate estimates of the leading eigensurfaces. The diagonal shapes of the true leading eigenfunctions indicate strong nonseparability features in the covariance function, features which are not captured by the Product FPCA model. The eigensurfaces have such diagonal shapes because they are polynomials of the sum  $s_1 + s_2$ , and later eigensurfaces change faster along the input domain because they are polynomials of higher order.

Finally, Fig. 5 shows that, when using more than two components, NSGP is the preferable model in terms of explaining better the main modes of variation in the data.

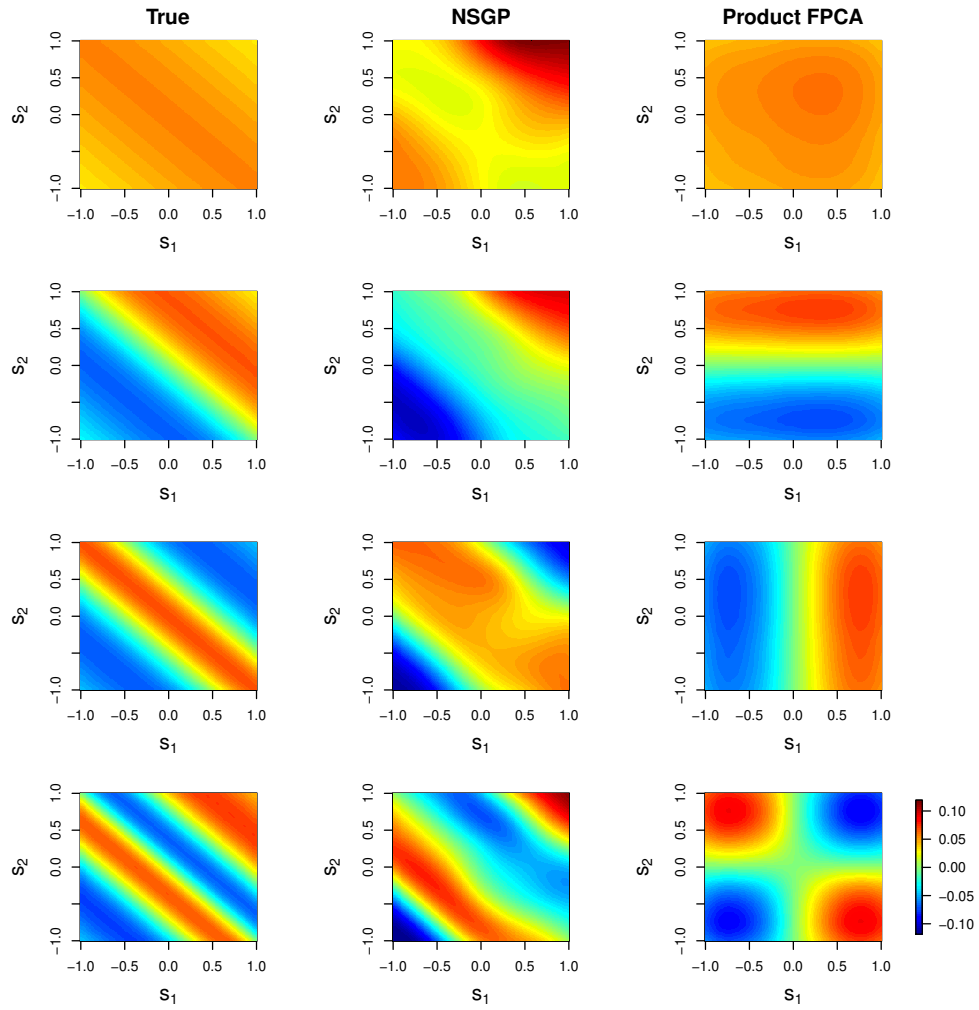


**Fig. 4.** First four leading eigensurfaces  $\phi(s_1, s_2)$  of the true model (left column) and the corresponding estimated eigensurfaces  $\hat{\phi}(s_1, s_2)$  from the NSGP model (centre) and Product FPCA model (right). Chebyshev polynomials data.



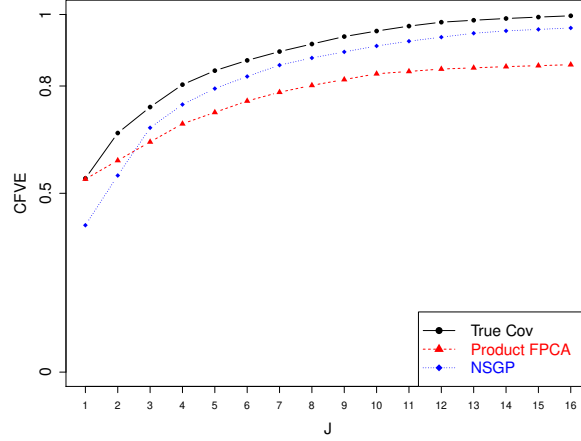


**Fig. 5.** Comparison of cumulative FVEs obtained by the true, and Product FPCA, and NSGP models. Chebyshev polynomials data.

## 5 Application

In this application, we model the daily mean temperature data observed from 01-01-1998 to 31-12-2005 in 36 stations in Canada. The dataset was obtained by using the R package `weathercan` (LaZerte and Albers, 2018), which was employed to download the data from the Environment and Climate Change Canada (2019) website. The data corresponding to a year is assumed to be a realisation of a random process, so that we have eight realisations.

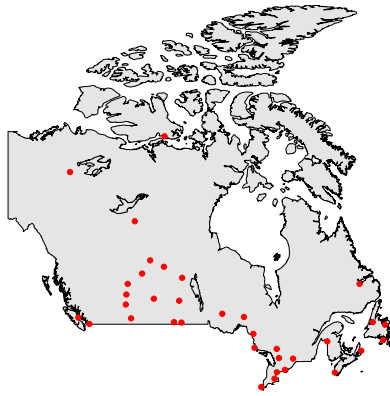
We use equation (1) to model the daily mean temperature  $X$ , where  $f(\cdot)$  follows a GP with covariance function (8) and squared exponential correlation function  $g(\cdot)$ . The coordinate directions are  $\mathbf{t} = (\tau, s_1, s_2)^\top$ , corresponding to time, latitude and longitude, respectively. For each realisation (year), the mean function  $\mu(\tau)$  was taken to be the sample mean across the 36 stations. The parameters  $\theta$  are assumed to be time-varying and we use a B-spline basis system with six regularly spaced knots to model them.

The estimate of the overall standard deviation  $\sigma(\tau)$  can be seen in Fig. 8, indicating that in winter months there is a higher variation in the temperature data relative to the mean function across the stations, what can be noticed in the mean temperature data (see Fig. 7).

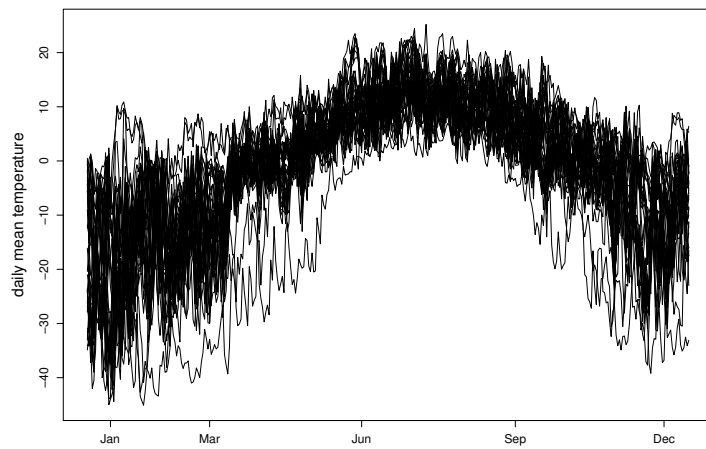
The estimates for the elements of the varying matrix  $\Sigma(\tau)$  are shown in Fig. 9. The change of parameter values over time indicate that the fluctuation of the process over each direction is different for different times of the year, something that stationary models cannot capture. Moreover, the departure from 0 of the directions of dependence  $\rho_{pq}, p \neq q$ , reveals the presence of interaction between the coordinate directions, showing nonseparable features in the covariance structure.

Fig. 10 shows the empirical and the NSGP covariance functions estimates of  $\text{Cov}[X(\tau_0, s_1, s_2), X(\tau_0, s'_1, s'_2)]$  for three different days  $\tau_0$  of the year, whose season is summer (left), autumn (middle) and winter (right). The coordinates  $s'_1 = 49.03$  and  $s'_2 = -122.36$  correspond to a station located in the province of British Columbia. The plots of the empirical covariance

functions show a larger variation across stations as we get closer to the winter, and this nonstationary feature is captured by the NSGP model.



**Fig. 6.** Map of Canada and the location of 36 stations where the data were observed.



**Fig. 7.** Daily mean temperature of 36 canadian stations in 2005.

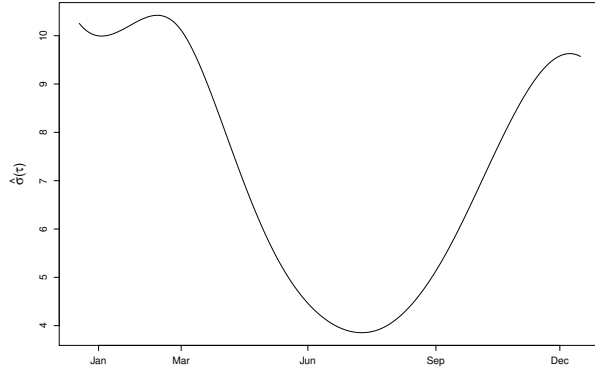


**Fig. 8.** Estimate of  $\sigma(\tau)$ .

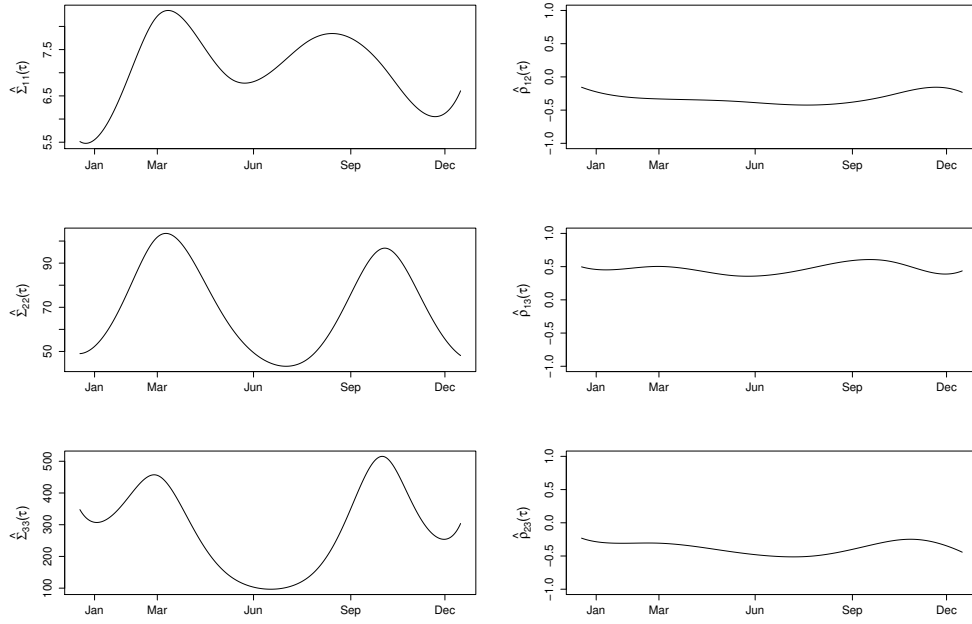


**Fig. 9.** Estimates of diagonal elements of varying anisotropy matrix  $\Sigma$  (left) and of directions of dependence  $\rho_{pq} = \Sigma_{pq} / \sqrt{\Sigma_{pp}\Sigma_{qq}}$  (right).

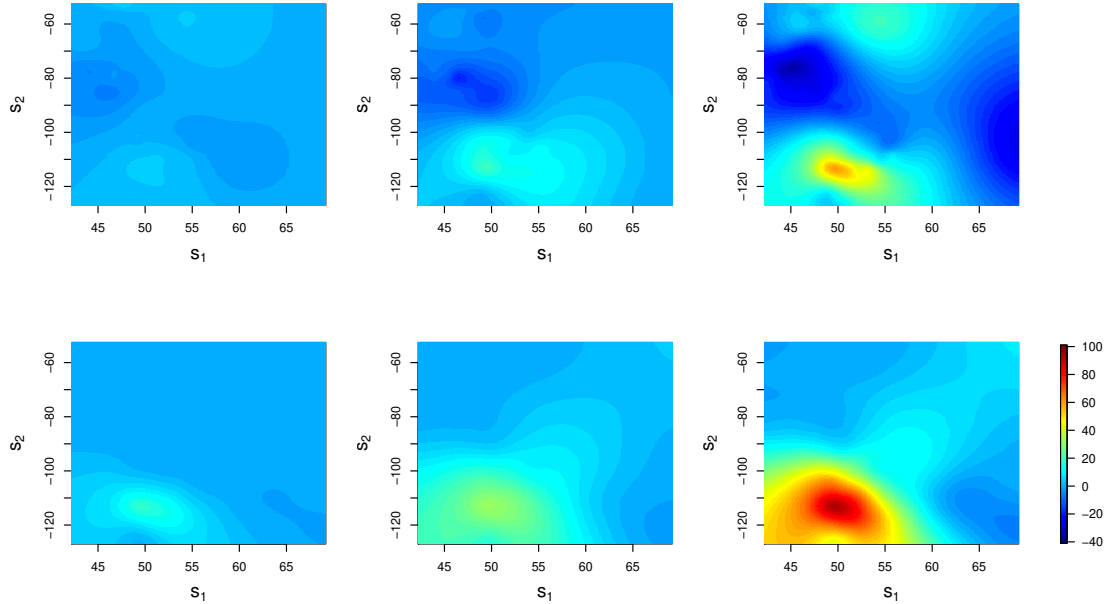


**Fig. 10.** Empirical covariance function (top) and NSGP covariance function (bottom) estimates of  $\text{Cov}[X(\tau = \tau_0, s_1, s_2), X(\tau' = \tau_0, s'_1 = 49.03, s'_2 = -122.36)]$  for different days of the year:  $\tau_0 = 180^{\text{th}}$  day (left),  $\tau_0 = 270^{\text{th}}$  day (middle),  $\tau_0 = 365^{\text{th}}$  day (right).

## 6 Discussion

Whereas nonparametric models for the covariance function are flexible but difficult to estimate in multidimensional domains due to the curse of dimensionality problem, parametric models can easily be estimated but their flexibility is limited by the choice of parametric covariance function, which is usually either stationary or separable. We propose to use a flexible, convolution-based approach which allows for nonstationarity and nonseparability, crucial properties to achieve good fit of the covariance function, extract the most important modes of variation in the data and obtain better estimates of uncertainty in predictions. This approach is readily applied to multidimensional domains.

The unconstrained estimation of the parameters in the varying anisotropy matrix enables us to model them as a function of time or spatial location easily. They can be further modelled as a function of time (or spatially) dependent covariates or other covariates which bring information for each subject. In any of these cases, the function can be represented by a variety of basis functions, among which we have found B-splines basis very suitable for ensuring smoothness and being flexible.

In particular, our proposed spherical parametrisation for  $\Sigma_{Q \times Q}(\mathbf{t})$ , which allows us to easily deal with input dimensions higher than two, is specified by a decomposition whose parameters have statistical interpretation. This is important for many applications. For example, if random trajectories fluctuate over time more quickly in the winter than in other seasons (see, for example,

the application to Canadian temperature data), then time (or a time-dependent covariate) seems a natural input for the corresponding length-scale parameter. The spherical parametrisation might also be helpful if we wish to conduct inference on those parameters.

A final remark on the estimation of  $\tau$ -varying parameters using B-splines in equation (9) is that when we use all the data (rather than using local likelihood estimation (LLE)), this of course requires a potentially high computational cost. However, when computational costs are not prohibitive, this approach should be preferable to the local likelihood approach, whose performance heavily depends on the neighbourhood size  $r$ . In the LLE, if a small neighbourhood is used (e.g. in order to model very local features), one might obtain unstable local estimates. On the other hand, if a large neighbourhood is used (something necessary when data are sparse), then the local stationarity assumption may be no longer appropriate and the local estimates might be very biased.

Instead of using empirical Bayes estimates, we could have defined a hyperprior distribution for  $\theta$ . In this case, our knowledge (posterior distribution) about  $\theta$  is updated as more data are observed. Finding the mode of the posterior density is a way to find what we call the *maximum a posteriori* (MAP) estimate of  $\theta$ . When we use a non-informative or a uniform prior distribution, the MAP estimates are precisely the same as the empirical Bayes estimates (Shi and Choi, 2011).

The decomposition of GPs may be important for developing efficient approximation for big data, non-Gaussian data (Wang and Shi, 2014) and heavy-tailed data (Shah et al., 2014; Wang et al., 2017; Cao et al., 2018). For non-Gaussian and heavy-tailed data, the decomposition might be used instead of their predictive distributions which are usually complicated. It can also be important for further analysis of scalar-on-functions or function-on-functions regression models, where we try to reduce the dimension of data by using a small number of components. Our proposed approach can be especially important when these components (eigensurfaces) are nonseparable, as we have seen in the simulation studies.

Convolution-based GP methods can be used to deal with multivariate GP outputs. For example, dependence between spatial processes is discussed in Ver Hoef and Barry (1998) and used by Boyle and Freaun (2004) to work with multiple outputs. Considering nonstationarity in the multivariate setting is a topic for future research.

## References

- Allen, G. I., Grose, L., and Taylor, J. (2014). A generalized least-square matrix decomposition. *Journal of the American Statistical Association*, 109(505):145–159.
- Aston, J. A., Pigoli, D., Tavakoli, S., et al. (2017). Tests for separability in nonparametric covariance operators of random surfaces. *The Annals of Statistics*, 45(4):1431–1461.
- Ba, S. and Joseph, V. R. (2012). Composite Gaussian process models for emulating expensive functions. *Ann. Appl. Stat.*, 6(4):1838–1860.
- Banerjee, S., Carlin, B. P., and Gelfand, A. E. (2015). *Hierarchical modeling and analysis for spatial data*. CRC Press, 2nd edition.

- Basawa, I. V. and Prakasa Rao, B. L. S. (1980). *Statistical Inference for Stochastic Processes*. Academic Press.
- Bosq, D. (2000). *Linear Processes in Function Spaces: Theory and Applications*. Lectures notes in statistics, Springer Verlag.
- Boyle, P. and Frean, M. (2004). Dependent Gaussian processes. In *Advances in neural information processing systems*, pages 217–224.
- Calandra, R., Peters, J., Rasmussen, C. E., and Deisenroth, M. P. (2016). Manifold Gaussian processes for regression. In *Neural Networks (IJCNN), 2016 International Joint Conference on*, pages 3338–3345. IEEE.
- Cao, C., Shi, J. Q., and Lee, Y. (2018). Robust functional regression model for marginal mean and subject-specific inferences. *Statistical Methods in Medical Research*, 27(11):3236–3254.
- Cappello, C., De Iaco, S., and Posa, D. (2018). Testing the type of non-separability and some classes of space-time covariance function models. *Stochastic Environmental Research and Risk Assessment*, 32(1):17–35.
- Carlin, B. P. and Louis, T. A. (2008). *Bayesian methods for data analysis*. CRC Press.
- Chen, K., Delicado, P., and Müller, H.-G. (2017). Modelling function-valued stochastic processes, with applications to fertility dynamics. *Journal of the Royal Statistical Society: Series B (Statistical Methodology)*, 79(1):177–196.
- Chen, K. and Müller, H.-G. (2012). Modeling repeated functional observations. *Journal of the American Statistical Association*, 107(500):1599–1609.
- Constantinou, P., Kokoszka, P., and Reimherr, M. (2017). Testing separability of space-time functional processes. *Biometrika*, 104(2):425–437.
- Cressie, N. and Huang, H.-C. (1999). Classes of nonseparable, spatio-temporal stationary covariance functions. *Journal of the American Statistical Association*, 94(448):1330–1339.
- de Boor, C. (2001). *A Practical Guide to Splines*. New York: Springer.
- De Iaco, S., Myers, D. E., and Posa, D. (2002). Nonseparable space-time covariance models: some parametric families. *Mathematical Geology*, 34(1):23–42.
- Deisenroth, M. and Ng, J. W. (2015). Distributed Gaussian Processes. In Bach, F. and Blei, D., editors, *Proceedings of the 32nd International Conference on Machine Learning*, volume 37 of *Proceedings of Machine Learning Research*, pages 1481–1490, Lille, France. PMLR.
- Dunlop, M. M., Girolami, M. A., Stuart, A. M., and Teckentrup, A. L. (2018). How Deep Are Deep Gaussian Processes? *Journal of Machine Learning Research*, 19(54):1–46.

- Environment and Climate Change Canada (2019). Historical Data. [Online; accessed 3-January-2019].
- Gneiting, T. (2002). Nonseparable, stationary covariance functions for space–time data. *Journal of the American Statistical Association*, 97(458):590–600.
- Hall, P., Müller, H.-G., , and Yao, F. (2008). Modelling sparse generalized longitudinal observations with latent gaussian processes. *Journal of the Royal Statistical Society. Series B (Methodological)*, 70.
- Higdon, D. (1998). A process-convolution approach to modelling temperatures in the North Atlantic Ocean. *Environmental and Ecological Statistics*, 5(2):173–190.
- Higdon, D. (2002). Space and space-time modeling using process convolutions. In *Quantitative methods for current environmental issues*, pages 37–56. Springer.
- Higdon, D., Swall, J., and Kern, J. (1999). Non-stationary spatial modeling. *Bayesian statistics*, 6(1):761–768.
- Horváth, L. and Kokoszka, P. (2012). *Inference for functional data with applications*, volume 200. Springer Science & Business Media.
- Jidling, C., Wahlström, N., Wills, A., and Schön, T. B. (2017). Linearly constrained Gaussian processes. In Guyon, I., Luxburg, U. V., Bengio, S., Wallach, H., Fergus, R., Vishwanathan, S., and Garnett, R., editors, *Advances in Neural Information Processing Systems 30*, pages 1215–1224. Curran Associates, Inc.
- Kanagawa, M., Hennig, P., Sejdinovic, D., and Sriperumbudur, B. K. (2018). Gaussian processes and kernel methods: A review on connections and equivalences. *arXiv preprint arXiv:1807.02582*.
- LaZerte, S. E. and Albers, S. (2018). weathercan: Download and format weather data from Environment and Climate Change Canada. *The Journal of Open Source Software*, 3(22):571.
- Leng, C., Zhang, W., and Pan, J. (2010). Semiparametric mean–covariance regression analysis for longitudinal data. *Journal of the American Statistical Association*, 105(489):181–193.
- Liu, H., Cai, J., Ong, Y.-S., and Wang, Y. (2018). Understanding and Comparing Scalable Gaussian Process Regression for Big Data. *arXiv preprint arXiv:1811.01159*.
- O’Hagan, A. and Kingman, J. F. C. (1978). Curve fitting and optimal design for prediction (with discussion). *Journal of the Royal Statistical Society. Series B (Methodological)*, 40(1):1–42.
- Paciorek, C. J. and Schervish, M. J. (2006). Spatial modelling using a new class of nonstationary covariance functions. *Environmetrics*, 17(5):483–506.
- Pinheiro, J. C. and Bates, D. M. (1996). Unconstrained parametrizations for variance-covariance matrices. *Statistics and computing*, 6(3):289–296.

- Pourahmadi, M. (1999). Joint mean-covariance models with applications to longitudinal data: Unconstrained parameterisation. *Biometrika*, 86(3):677–690.
- Ramsay, J. and Silverman, B. W. (2005). *Functional Data Analysis*. Springer, 2 edition.
- Rapisarda, F., Brigo, D., and Mercurio, F. (2007). Parameterizing correlations: a geometric interpretation. *IMA Journal of Management Mathematics*, 18(1):55–73.
- Rasmussen, C. and Williams, C. (2006). *Gaussian Processes for Machine Learning*. University Press Group Limited.
- Risser, M. and Calder, C. (2017). Local Likelihood Estimation for Covariance Functions with Spatially-Varying Parameters: The convoSPAT Package for R. *Journal of Statistical Software, Articles*, 81(14):1–32.
- Rougier, J. (2017). A representation theorem for stochastic processes with separable covariance functions, and its implications for emulation. *arXiv preprint arXiv:1702.05599*.
- Sampson, P. D. and Guttorp, P. (1992). Nonparametric estimation of nonstationary spatial covariance structure. *Journal of the American Statistical Association*, 87(417):108–119.
- Shah, A., Wilson, A., and Ghahramani, Z. (2014). Student-t Processes as Alternatives to Gaussian Processes. In Kaski, S. and Corander, J., editors, *Proceedings of the Seventeenth International Conference on Artificial Intelligence and Statistics*, volume 33 of *Proceedings of Machine Learning Research*, pages 877–885, Reykjavik, Iceland. PMLR.
- Shi, J. Q. and Choi, T. (2011). *Gaussian process regression analysis for functional data*. CRC Press.
- Stein, M. L. (1999). *Interpolation of Spatial Data: Some Theory for Kriging*. Springer: NY.
- Stein, M. L. (2005). Space–time covariance functions. *Journal of the American Statistical Association*, 100(469):310–321.
- Sung, C.-L., Hung, Y., Rittase, W., Zhu, C., and Wu, C. (2017). A generalized Gaussian process model for computer experiments with binary time series. *arXiv preprint arXiv:1705.02511*.
- Tibshirani, R. and Hastie, T. (1987). Local likelihood estimation. *Journal of the American Statistical Association*, 82(398):559–567.
- Tran, D., Ranganath, R., and Blei, D. M. (2015). The variational Gaussian process. *arXiv preprint arXiv:1511.06499*.
- van der Wilk, M., Rasmussen, C. E., and Hensman, J. (2017). Convolutional Gaussian Processes. In Guyon, I., Luxburg, U. V., Bengio, S., Wallach, H., Fergus, R., Vishwanathan, S., and Garnett, R., editors, *Advances in Neural Information Processing Systems 30*, pages 2849–2858. Curran Associates, Inc.



- Ver Hoef, J. M. and Barry, R. P. (1998). Constructing and fitting models for cokriging and multivariable spatial prediction. *Journal of Statistical Planning and Inference*, 69(2):275–294.
- Wahba, G. (1990). *Spline models for observational data*, volume 59. Siam.
- Wang, B. and Shi, J. Q. (2014). Generalized Gaussian process regression model for non-Gaussian functional data. *Journal of the American Statistical Association*, 109(507):1123–1133.
- Wang, B. and Xu, A. (2019). Gaussian process methods for nonparametric functional regression with mixed predictors. *Computational Statistics & Data Analysis*, 131:80–90. High-dimensional and functional data analysis.
- Wang, Z., Shi, J. Q., and Lee, Y. (2017). Extended  $t$ -process regression models. *Journal of Statistical Planning and Inference*, 189:38 – 60.
- Yao, F., Müller, H.-G., and Wang, J.-L. (2005). Functional data analysis for sparse longitudinal data. *Journal of the American Statistical Association*, 100(470):577–590.
- Zhang, B., Sang, H., and Huang, J. Z. (2019). Smoothed Full-Scale Approximation of Gaussian Process Models for Computation of Large Spatial Datasets. *Statistica Sinica*.
- Zhang, W., Leng, C., and Tang, C. Y. (2015). A joint modelling approach for longitudinal studies. *Journal of the Royal Statistical Society: Series B (Statistical Methodology)*, 77(1):219–238.

## A Appendices

### A.1 Proof of Theorem 1

We show that

$$\begin{aligned}
& E \left[ \left\| X^c(\mathbf{t}) - \sum_{j=1}^J g_j(\mathbf{t}) \xi_j^* \right\|^2 \right] \\
&= E \langle X^c(\cdot) - \sum_{j=1}^J g_j(\cdot) \xi_j^*, X^c(\cdot) - \sum_{j=1}^J g_j(\cdot) \xi_j^* \rangle \\
&= E \left[ \langle X^c(\cdot), X^c(\cdot) \rangle - \sum_{j=1}^J (\langle X^c(\cdot), g_j(\cdot) \rangle)^2 \right] \\
&= E \|X^c\|^2 - \sum_{j=1}^J E \left[ \int_{\mathcal{T}} \int_{\mathcal{T}} X^c(\mathbf{t}) X^c(\mathbf{t}') g_j(\mathbf{t}) g_j(\mathbf{t}') dt dt' \right] \\
&= E \|X^c\|^2 - \sum_{j=1}^J \int_{\mathcal{T}} \int_{\mathcal{T}} k(\mathbf{t}, \mathbf{t}') g_j(\mathbf{t}) g_j(\mathbf{t}') dt dt'
\end{aligned}$$

$$= E\|X^c\|^2 - \sum_{j=1}^J \langle \Phi(g_j), g_j \rangle.$$

Hence, the minimising problem (17) becomes to maximise  $\sum_{j=1}^J \langle \Phi(g_j), g_j \rangle$  with respect to  $g_1, \dots, g_J \in L^2(\mathcal{T})$ . Since the operator  $\Phi$  is symmetric, positive definite Hilbert-Schmidt, following Theorem 3.2 in Horváth and Kokoszka (2012) the proof is completed.

## A.2 Proof of Theorem 2

Without loss of generality, we consider  $Q = 2$ . Then  $\mathbf{t} = (s, \tau)^\top$  with  $s, \tau \in \mathbb{R}$ . Let  $\{\hat{\lambda}_j, j = 1, 2, \dots\}$  and  $\{\hat{\phi}_j(\cdot), j = 1, 2, \dots\}$  be the eigenvalues and eigenfunctions of the covariance function  $\hat{k}(\mathbf{t}, \mathbf{t}') = k_{\hat{\theta}}(\mathbf{t}, \mathbf{t}')$ , where  $\mathbf{t} = (s, \tau)^\top$ ,  $\mathbf{t}' = (s', \tau')^\top$ , and

$$\hat{\xi}_j = \langle X^c(\cdot), \hat{\phi}_j(\cdot) \rangle = \int X^c(\mathbf{t}) \hat{\phi}_j(\mathbf{t}) dt.$$

Let  $p(\mathbf{x}_l^c; \boldsymbol{\theta}) = p(x_1^c, \dots, x_l^c; \boldsymbol{\theta})$  be the density function of  $\mathbf{x}_l^c$ . Let  $\boldsymbol{\theta}_0$  be the true value of  $\boldsymbol{\theta}$  and  $p_l(\boldsymbol{\theta})$  be the conditional density of  $\mathbf{x}_l^c$  for given  $\mathbf{x}_{l-1}^c$ . Actually, for every  $l \geq 1$ ,

$$p_l(\boldsymbol{\theta}) = p(\mathbf{x}_l^c; \boldsymbol{\theta}) / p(\mathbf{x}_{l-1}^c; \boldsymbol{\theta}).$$

It shows that  $p_l(\boldsymbol{\theta}) = N(\mu_{l|l-1}, \sigma_{l|l-1}^2)$  with

$$\mu_{l|l-1} = \mathbf{k}_l \mathbf{K}_{l-1}^{-1} \mathbf{x}_{l-1}^c, \quad \sigma_{l|l-1}^2 = k(\mathbf{t}_l, \mathbf{t}_l) - \mathbf{k}_l \mathbf{K}_{l-1}^{-1} \mathbf{k}_l^\top,$$

where  $\mathbf{k}_l = (k(\mathbf{t}_1, \mathbf{t}_l), \dots, k(\mathbf{t}_{l-1}, \mathbf{t}_l))^\top$ . Assume that  $p_l(\boldsymbol{\theta})$  is twice differentiable with respect to  $\boldsymbol{\theta}$ . Let  $\phi_l(\boldsymbol{\theta}) = \log p_l(\boldsymbol{\theta})$ ,  $\mathbf{U}_l(\boldsymbol{\theta}) = \dot{\phi}_l(\boldsymbol{\theta})$  and  $\mathbf{V}_l(\boldsymbol{\theta}) = \ddot{\phi}_l(\boldsymbol{\theta})$ , where  $\dot{g}$  and  $\ddot{g}$  are the first and second derivatives of function  $g(\boldsymbol{\theta})$  with respect to  $\boldsymbol{\theta}$ , respectively. Without loss of generality, we consider the parameter with one dimension. Then  $\mathbf{U}_l(\boldsymbol{\theta})$  and  $\mathbf{V}_l(\boldsymbol{\theta})$  are scalars  $U_l(\boldsymbol{\theta})$  and  $V_l(\boldsymbol{\theta})$ , and denoted by  $U_l = U_l(\boldsymbol{\theta}_0)$  and  $V_l = V_l(\boldsymbol{\theta}_0)$ . For the proof of Theorem 2, we need the following conditions:

(C1)  $\sup_{s, \tau} |\mu(s, \tau)| < \infty$ .

(C2) The covariance function  $k_\theta(\mathbf{t}, \mathbf{t}')$  has thrice continuous derivative with respect to  $\theta$ , and is continuous, differentiable and square-integrable on  $\mathbf{t}, \mathbf{t}'$ . For eigenvalues and eigenvectors of  $k_\theta$ , assume  $\delta_j > 0$  and  $\phi_j(s, \tau)$  is square-integrable, where  $\delta_j = \min\{\lambda_1 - \lambda_2, \lambda_{j-1} - \lambda_j, \lambda_j - \lambda_{j+1}\}$ .

Define  $i_k(\theta_0) = \text{Var}[U_k | \mathcal{F}_{k-1}] = E[U_k^2 | \mathcal{F}_{k-1}]$ , where  $\mathcal{F}_{k-1} = \sigma(x_1^c, \dots, x_{l-1}^c)$ . Let  $I_n(\theta_0) = \sum_{k=1}^n i_k(\theta_0)$ ,  $S_n = \sum_{k=1}^n U_k$  and  $S_n^* = \sum_{k=1}^n V_k + I_n(\theta_0)$ . It shows that  $S_n$  and  $S_n^*$  are zero-mean martingales with respect to  $\sigma$ -filtration  $\mathcal{F}_n$ . The third condition is

(C3) Assume

1.  $n^{-1} |\sum_{k=1}^n V_k| \xrightarrow{P} i(\theta_0)$ , and  $n^{-1/2} S_n \xrightarrow{L} N(0, i(\theta_0))$  for some non-random function  $i(\theta_0) > 0$ ,
2. For all  $\varepsilon > 0$  and  $\eta > 0$ , there exists  $\delta > 0$  and  $n_0 > 0$  such that for all  $n > n_0$ ,  $P\{n^{-1} |\sum_{k=1}^n (V(\theta) - V_k)| > \eta, |\theta - \theta_0| < \delta\} < \varepsilon$ ,

3.  $n^{-1} \sum_{k=1}^n E|W_k(\theta)| < M < \infty$  for all  $\theta$  and  $n$ , where  $W_k(\theta)$  is the third derivative of  $\phi_k(\theta)$  with respect to  $\theta$ .

Under conditions (C2) and (C3), one can easily show that the conditions of Theorem 2.2 in Chapter 7 of Basawa and Prakasa Rao (1980) holds. Hence,  $\hat{\theta}$  is a consistent estimator of  $\theta_0$  and has asymptotically normality,

$$n^{-1/2}(\hat{\theta} - \theta_0) \xrightarrow{L} N(0, i(\theta_0)^{-1}),$$

which indicates that

$$\|\hat{\theta} - \theta_0\| = O_p(\{\log(n)/n\}^{1/2}).$$

Since the covariance function  $k_\theta$  is thrice continuously differentiate on  $\theta$ , we have

$$\|k_{\hat{\theta}}(\cdot, \cdot) - k_\theta(\cdot, \cdot)\| = O_p(\{\log(n)/n\}^{1/2}).$$

From Lemma 4.2 in Bosq (2000), it follows that for all  $j$ ,

$$\|\hat{\lambda}_j - \lambda_j\| \leq \|k_{\hat{\theta}}(\cdot, \cdot) - k_\theta(\cdot, \cdot)\|, \quad (19)$$

and similar to Lemma 4.3 in Bosq (2000), we have, for fixed  $j$ ,

$$\|\hat{\phi}_j(\cdot) - \phi_j(\cdot)\| \leq 2\sqrt{2}\delta_j^{-1}\|k_{\hat{\theta}}(\cdot, \cdot) - k_\theta(\cdot, \cdot)\|, \quad (20)$$

where  $\delta_j = \min\{\lambda_1 - \lambda_2, \lambda_{j-1} - \lambda_j, \lambda_j - \lambda_{j+1}\}$ . Then (19) and (20) give that

$$\begin{aligned} \|\hat{\lambda}_j - \lambda_j\| &= O_p(\{\log(n)/n\}^{1/2}), \\ \|\hat{\phi}_j(\cdot) - \phi_j(\cdot)\| &= O_p(\{\log(n)/n\}^{1/2}). \end{aligned}$$

For  $\hat{\xi}_j$ , we show that

$$\begin{aligned} |\hat{\xi}_j - \xi| &= \left| \int (Z(s, \tau) - \hat{\mu}(s, \tau)) \hat{\phi}_j(s, \tau) ds d\tau - \int (Z(s, \tau) - \mu(s, \tau)) \phi_j(s, \tau) ds d\tau \right| \\ &\leq \left| \int (Z(s, \tau) - \mu(s, \tau)) (\hat{\phi}_j(s, \tau) - \phi_j(s, \tau)) ds d\tau \right| \\ &\quad + \left| \int (\hat{\mu}(s, \tau) - \mu(s, \tau)) (\hat{\phi}_j(s, \tau) - \phi_j(s, \tau)) ds d\tau \right| \\ &\quad + \left| \int (\hat{\mu}(s, \tau) - \mu(s, \tau)) \phi_j(s, \tau) ds d\tau \right|. \end{aligned}$$

Hence, from condition (C2), (19) and  $\sup_{s, \tau} |\hat{\mu}(s, \tau) - \mu(s, \tau)| = O_p[\{\log(n)/n\}^{1/2}]$ , it shows that

$$\|\hat{\xi}_j - \xi\| = O_p(\{\log(n)/n\}^{1/2}).$$

### A.3 Proof of Theorem 3

Let  $\mathbf{K}_n = (k(\mathbf{t}_i, \mathbf{t}_j))_{n \times n}$  be a Gram matrix, and  $\lambda_1^{(n)} \geq \lambda_2^{(n)} \geq \dots \geq \lambda_n^{(n)} \geq 0$  be the eigenvalues of  $\mathbf{K}_n$ , and  $\mathbf{V}_{j,n}$ ,  $j = 1, \dots, n$  be the eigenvectors of  $\mathbf{K}_n$ . Then from the Nyström approximation method, we show that

$$\begin{aligned} \sqrt{n}V_{hj,n} &= \phi_j(\mathbf{t}_h) + O_p\left(\frac{1}{\sqrt{n}}\right), & \frac{\lambda_j^{(n)}}{n} &= \lambda_j + O_p\left(\frac{1}{\sqrt{n}}\right), \\ \frac{\sqrt{n}}{\lambda_j^{(n)}}\mathbf{k}_n^\top(\mathbf{t})\mathbf{V}_{j,n} &= \phi_j(\mathbf{t}) + O_p\left(\frac{1}{\sqrt{n}}\right), \end{aligned} \quad (21)$$

where  $V_{hj,n}$  is the  $h$ -th element of  $\mathbf{V}_{j,n}$ , and  $\mathbf{k}_n(\mathbf{t}) = (k(\mathbf{t}_1, \mathbf{t}), \dots, k(\mathbf{t}_n, \mathbf{t}))^\top$ . Due to  $E[\xi_j] = 0$  and  $\text{Var}[\xi_j] = \lambda_j \rightarrow 0$  as  $j \rightarrow \infty$ , it follows from (21) that

$$f_n(\mathbf{t}) = \sum_{j=1}^n \phi_j(\mathbf{t})\xi_j = \sum_{j=1}^n \frac{\sqrt{n}}{\lambda_j^{(n)}}\mathbf{k}_n^\top(\mathbf{t})\mathbf{V}_{j,n}\xi_j + o_p(1).$$

In addition, we show that

$$\begin{aligned} \xi_j &= \lambda_j \langle f, \phi_j \rangle \\ &= \lambda_j \langle f, \frac{\sqrt{n}}{\lambda_j^{(n)}}\mathbf{k}_n^\top(\cdot)\mathbf{V}_{j,n} \rangle + O_p\left(\frac{1}{\sqrt{n}}\right) \\ &= \frac{\sqrt{n}\lambda_j}{\lambda_j^{(n)}}\mathbf{V}_{j,n}^\top \langle f, \mathbf{k}_n(\cdot) \rangle + O_p\left(\frac{1}{\sqrt{n}}\right) \\ &= \frac{\sqrt{n}\lambda_j}{\lambda_j^{(n)}}\mathbf{V}_{j,n}^\top \mathbf{f} + O_p\left(\frac{1}{\sqrt{n}}\right). \end{aligned}$$

Hence, we have

$$\begin{aligned} f_n(\mathbf{t}) &= \sum_{j=1}^n \frac{\sqrt{n}}{\lambda_j^{(n)}}\mathbf{k}_n^\top(\mathbf{t})\mathbf{V}_{j,n} \frac{\sqrt{n}\lambda_j}{\lambda_j^{(n)}}\mathbf{V}_{j,n}^\top \mathbf{f} + o_p(1) \\ &= \mathbf{k}_n^\top(\mathbf{t}) \sum_{j=1}^n \frac{1}{\lambda_j^{(n)}}\mathbf{V}_{j,n}\mathbf{V}_{j,n}^\top \mathbf{f} + o_p(1) \\ &= \mathbf{k}_n^\top(\mathbf{t})\mathbf{K}_n^{-1} \mathbf{f} + o_p(1), \end{aligned}$$

which indicates that  $E[f(\mathbf{t})|\mathbf{f}] = \mathbf{k}_n^\top(\mathbf{t})\mathbf{K}_n^{-1} \mathbf{f} = f_n(\mathbf{t}) + o_p(1)$ .

The Nyström approximation is also applied to  $X(\mathbf{t})$  and  $\varepsilon(\mathbf{t})$ , respectively, and we have

$$\begin{aligned} X_n(\mathbf{t}) &= \tilde{\mathbf{k}}_n^\top(\mathbf{t})\tilde{\mathbf{K}}_n^{-1} \mathbf{x} + o_p(1), \\ \varepsilon_n(\mathbf{t}) &= \mathbf{k}_{\varepsilon_n}^\top(\mathbf{t})\mathbf{K}_{\varepsilon_n}^{-1} \boldsymbol{\varepsilon} + o_p(1), \end{aligned}$$

where  $\mathbf{x} = (x(\mathbf{t}_1), \dots, x(\mathbf{t}_n))^\top$ ,  $\boldsymbol{\varepsilon} = (\varepsilon(\mathbf{t}_1), \dots, \varepsilon(\mathbf{t}_n))^\top$ ,  $\tilde{k} = k + k_\varepsilon$ ,  $[\tilde{\mathbf{K}}_n]_{ij} = \tilde{k}(\mathbf{t}_i, \mathbf{t}_j)$ ,  $\tilde{\mathbf{k}}_n(\mathbf{t}) = (\tilde{k}(\mathbf{t}_1, \mathbf{t}), \dots, \tilde{k}(\mathbf{t}_n, \mathbf{t}))^\top$ ,  $[\mathbf{K}_{\varepsilon n}]_{ij} = k_\varepsilon(\mathbf{t}_i, \mathbf{t}_j)$ , and  $\mathbf{k}_{\varepsilon n}(\mathbf{t}) = (k_\varepsilon(\mathbf{t}_1, \mathbf{t}), \dots, k_\varepsilon(\mathbf{t}_n, \mathbf{t}))^\top$ . From the definition of  $k_\varepsilon$ , we know that  $\mathbf{k}_{\varepsilon n}(\mathbf{t}) = \mathbf{0}$  and  $\tilde{\mathbf{K}}_n = \mathbf{K}_n + \sigma_\varepsilon^2 \mathbf{I}_n$ . Hence, it follows that

$$f_n(\mathbf{t}) = X_n(\mathbf{t}) - \varepsilon_n(\mathbf{t}) = \mathbf{k}_n^\top(\mathbf{t})(\mathbf{K}_n + \sigma_\varepsilon^2 \mathbf{I}_n)^{-1} \mathbf{x} + o_p(1),$$

which suggests that

$$E[f(\mathbf{t})|\mathcal{D}] = \mathbf{k}_n^\top(\mathbf{t})(\mathbf{K}_n + \sigma_\varepsilon^2 \mathbf{I}_n)^{-1} \mathbf{x} = X_n(\mathbf{t}) + o_p(1).$$

## A.4 Additional simulation study

We simulate 30 realisations from a two-dimensional function-valued process  $X(\mathbf{t})$ ,  $\mathbf{t} = (\tau, s)^\top$ , observed at  $n_1 \times n_2 = 25 \times 25 = 625$  equally spaced points on  $[0, 1]^2$ . We assume a measurement error with variance  $\sigma_\varepsilon^2 = 0.1$  and the covariance function (8), with varying overall variance  $\sigma^2(\tau) = \exp(\tau)$  and varying anisotropy matrix  $\boldsymbol{\Sigma}(\tau) = \mathbf{C}^{1/2} \mathbf{R}(\tau) \mathbf{C}^{1/2}$ , where  $\mathbf{C} = \text{diag}(0.1, 0.1)$ ,  $\mathbf{R}_{11}(\tau) = \mathbf{R}_{22}(\tau) = 1$  and different specifications for  $\mathbf{R}_{12}(\tau) = \mathbf{R}_{21}(\tau)$ : we set  $\mathbf{R}_{12}(\tau) = 0$  to produce a separable covariance function and  $\mathbf{R}_{12}(\tau) = 0.95\tau$  and  $\mathbf{R}_{12}(\tau) = 0.8$  to produce non-separable ones. Four different specifications for  $g(\cdot)$  were used for generating the data: Matérn with  $\nu = 1/2$ ,  $\nu = 3/2$ ,  $\nu = 5/2$ , and  $\nu = 5$ .

Then we estimate the covariance structure by the NSGP model with two specifications for  $g(\cdot)$  (squared exponential and exponential) and by the Product FPCA model. In the NSGP model, the  $\tau$ -varying parameters are estimated via B-splines with 3 knots.

Figs 11 and 12 show the CFVEs obtained when the data generating processes is a GP and a  $T$ -process (with 6 degrees of freedom), respectively. The conclusions made for both figures are very similar, showing that the proposed NSGP approach is robust to heavy-tailed data.

Observe that the value of  $\mathbf{R}_{12}(\tau)$  measures how distant is the covariance structure from the separability assumption. Therefore, the top panel of figures show the separable case; the middle panel shows the case where the nonseparable feature is only strong when  $\tau$  is large; and the bottom panel show the case where the nonseparable feature is strong for any  $\tau$ . The figures indicate very similar performance of the three methods when the covariance is separable. However, when the nonseparable feature is strong, the NSGP models obtain better (or at least very similar) CFVEs than Product FPCA. In other words, when the covariance structure becomes more distant from the separability assumption, then the Product FPCA model seems to not capture important information about the variation in the data which are explained by nonseparable eigensurfaces. Observe, however, that the first eigensurface estimated by each method have very similar contribution, even in the strong nonseparability cases. This, of course, is because nonseparable features are caused by interaction between the coordinate directions, and therefore we do expect to see a clearer advantage of nonseparable models only in later eigensurfaces, not in the first one.

Whereas Matérn with  $\nu = 1/2$  is equivalent to the exponential kernel, Matérn with  $\nu = \infty$  converges to the squared exponential kernel. This explains why the exponential correlation kernel is preferable for data generated with small  $\nu$  and the squared exponential kernel provides better results for  $\nu = 5$ .

The larger the value of  $\nu$  the smoother are the random functions. Therefore, as we can see in the figures, the larger the value of  $\nu$ , the smaller is the number of components necessary to achieve a high CFVE. Each row of figures were not plotted using the same scale in order to visualise better the difference between the methods.

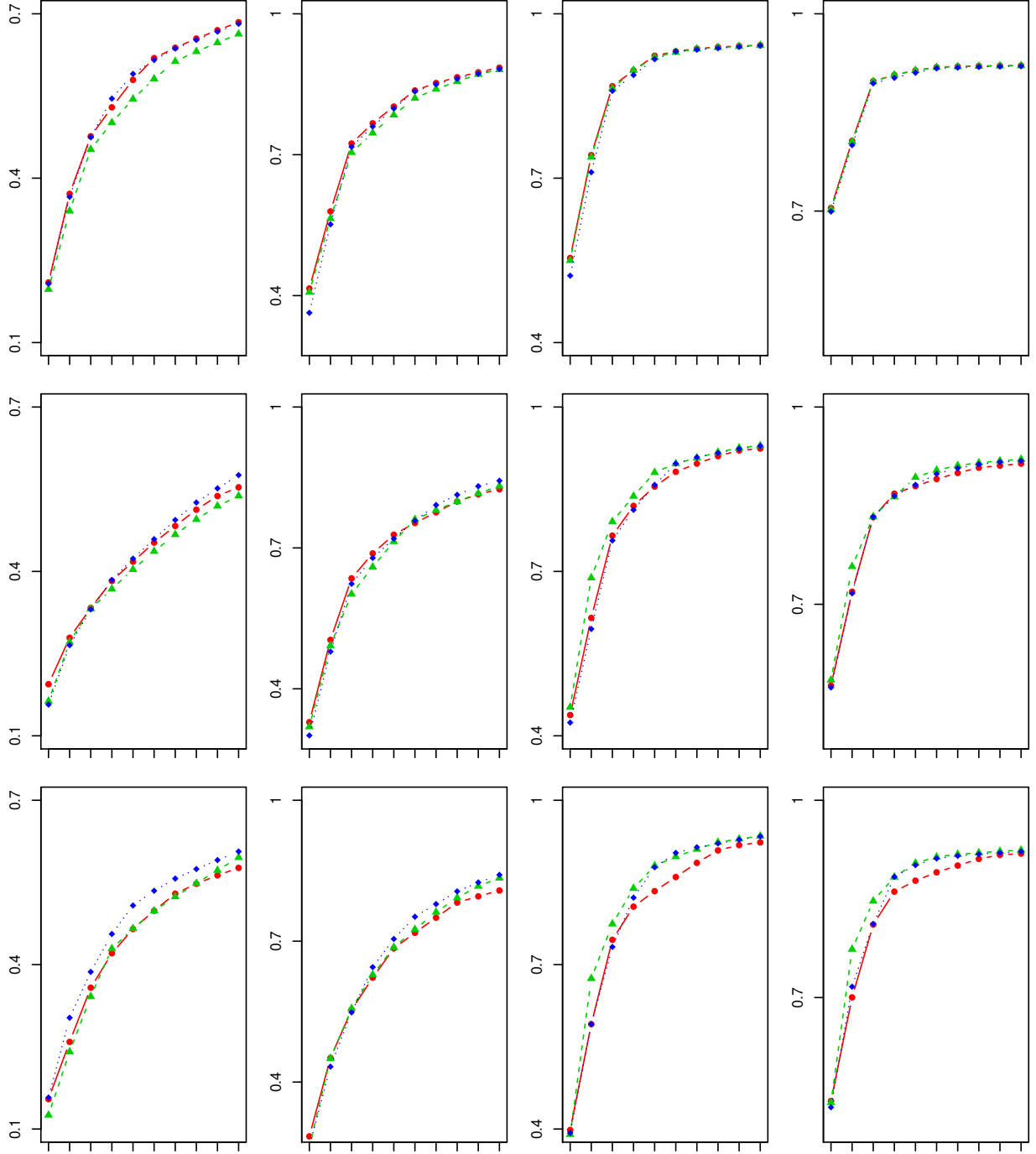


**Fig. 11.** CFVEs of GP data for  $J = 1, \dots, 10$ , obtained by Product FPCA (red), NSGP with squared exponential  $g(\cdot)$  (green), and NSGP with exponential  $g(\cdot)$  (blue). In each column, from the top to the bottom,  $\mathbf{R}_{12}(\tau) = 0$ ,  $\mathbf{R}_{12}(\tau) = 0.95\tau$ ,  $\mathbf{R}_{12}(\tau) = 0.8$ . In each row, from the left to the right, the data generating process follows a GP with covariance function (8), where  $g(\cdot)$  is Matérn with  $\nu = 1/2$ ,  $\nu = 3/2$ ,  $\nu = 5/2$ , and  $\nu = 5$ .

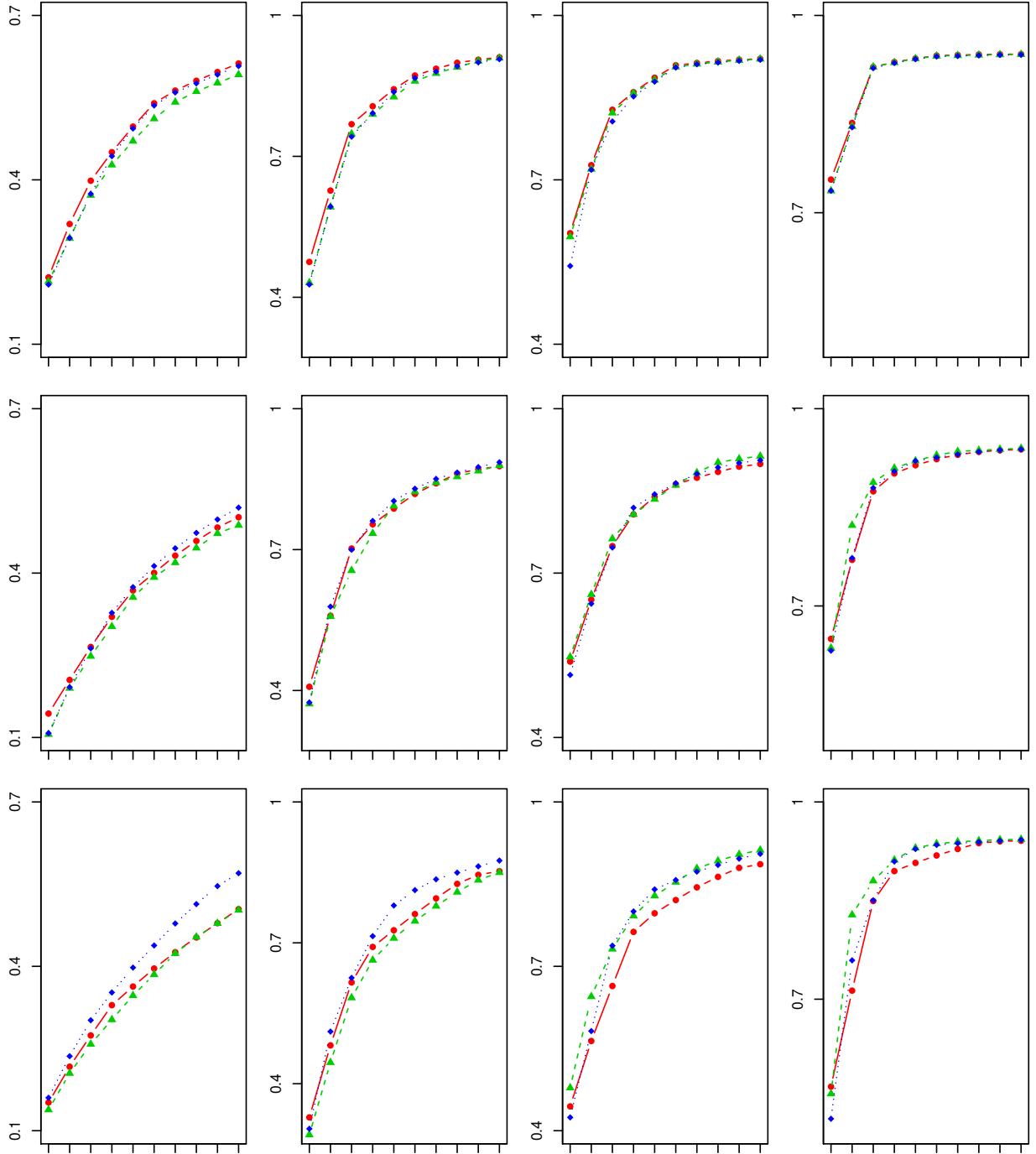


**Fig. 12.** CFVEs of  $T$ -process data for  $J = 1, \dots, 10$ , obtained by Product FPCA (red), NSGP with squared exponential  $g(\cdot)$  (green), and NSGP with exponential  $g(\cdot)$  (blue). In each column, from the top to the bottom,  $\mathbf{R}_{12}(\tau) = 0$ ,  $\mathbf{R}_{12}(\tau) = 0.95\tau$ ,  $\mathbf{R}_{12}(\tau) = 0.8$ . In each row, from the left to the right, the data generating process follows a  $T$ -process with covariance function (8), where  $g(\cdot)$  is Matérn with  $\nu = 1/2$ ,  $\nu = 3/2$ ,  $\nu = 5/2$ , and  $\nu = 5$ .